



Contents lists available at SciVerse ScienceDirect

Journal of Volcanology and Geothermal Research

journal homepage: www.elsevier.com/locate/jvolgeores

Surface deformation of Bezymianny Volcano, Kamchatka, recorded by GPS: The eruptions from 2005 to 2010 and long-term, long-wavelength subsidence

Ronni Grapenthin ^{a,*}, Jeffrey T. Freymueller ^a, Sergey S. Serovetnikov ^b

^a Geophysical Institute, University of Alaska Fairbanks, Fairbanks, AK, USA

^b Kamchatkan Branch of Geophysical Service of RAS, Petropavlovsk-Kamchatskiy, Russia

ARTICLE INFO

Article history:

Received 26 May 2012

Accepted 26 November 2012

Available online xxxx

Keywords:

Bezymianny

Volcano

Eruption

Volcano geodesy

Crustal deformation

Source modeling

ABSTRACT

Since Bezymianny Volcano resumed its activity in 1956, eruptions have been frequent; recently with up to 1–2 explosive events per year. To investigate deformation related to this activity we installed a GPS network of 8 continuous and 6 campaign stations around Bezymianny. The two striking observations for 2005–2010 are (1) rapid and continuous network-wide subsidence between 8 and 12 mm/yr, which appears to affect KAMNET stations more than 40 km away where we observe 4–5 mm/yr of subsidence, and (2) only the summit station BZ09 shows slight deviations from the average motion in the north component at times of eruptions.

The network-wide subsidence cannot be explained by tectonic deformation related to the build-up of interseismic strain due to subduction of the Pacific plate. A first order model of surface loading by eruptive products of the Kluchevskoy Group of Volcanoes also explains only a fraction of the subsidence. However, a deep sill at about 30 km under Kluchevskoy that constantly discharges material fits our observations well. The sill is constrained by deep seismicity which suggests 9.5 km width, 12.7 km length, and a 13° dip-angle to the south-east. We infer a closing rate of 0.22 m/yr, which implies a volume loss of 0.027 km³/yr (0.16 m/yr and 0.019 km³/yr considering surface loading). Additional stations in the near and far field are required to uniquely resolve the spatial extent and likely partitioning of this source.

We explain the eruption related deformation at BZ09 with a very shallow reservoir, likely within Bezymianny's edifice at a depth between 0.25 km and 1.5 km with a volume change of 1–4 × 10⁻⁴ km³. Much of the material erupted at Bezymianny may be sourced from deeper mid-crustal reservoirs with co-eruptive volume changes at or below the detection limit of the GPS network. Installation of more sensitive instruments such as tiltmeters would allow resolving of subtle co-eruptive motion.

© 2012 Elsevier B.V. All rights reserved.

1. Introduction

The Bezymianny Volcano is part of the Kluchevskoy Group of Volcanoes (KGV) at the northern end of the Central Kamchatka Depression in Kamchatka, Russia (Fig. 1). The group is named after the Kluchevskoy Volcano, the tallest (4835 m) and most productive volcano in Eurasia (60 Gt/yr, which translates to about 0.023 km³/yr of basalt, (Fedotov et al., 2010)) about 10 km to the north-northeast of the Bezymianny Volcano. Tolbachik (Fig. 1), about 20 km to the southwest of Bezymianny, is another notable volcano of this group, because in 1975–76 it produced the largest basaltic eruption in Kamchatka in historical time (Fedotov and Markhinin, 1983; Fedotov et al., 2010).

Bezymianny itself is equally notable; after about 1000 years of dormancy this 11,000 year old volcano (Belousov et al., 2007) entered

a new period of activity that started with a catastrophic flank collapse and lateral blast eruption in 1956 (Gorshkov, 1959; Belousov et al., 2007). The resulting horseshoe shaped crater opens to the south-east (Fig. 1) and was quickly filled by a new dome (Malyshev, 2000). The dome now almost touches the crater walls, which it already exceeds in elevation, and formed a crater of its own (Carter et al., 2007).

The current activity of Bezymianny is characterized by roughly 1–2 explosive eruptions per year (e.g., Girina, this volume), which are accompanied by pyroclastic flows and small lava flows. Prior work on the system that feeds this activity suggests a deep reservoir at about 30 km depth below the Kluchevskoy Volcano (Fedotov et al., 2010; Koulovskoy et al., 2011, this volume). From there magma is suggested to migrate into more shallow, mid-crustal reservoirs beneath Kluchevskoy (Fedotov et al., 2010) and Bezymianny (Fedotov et al., 2010; Thelen et al., 2010). An additional very shallow magma or volatile region within the edifice of Bezymianny was suggested by Thelen et al. (2010). Their study, however, was limited to only 3 months of data in the latter half of 2007, so it remains unclear whether this is a transient or permanent feature. Studies of relatively insoluble/soluble gas species ratios observed in fumarole

* Corresponding author at: Berkeley Seismological Laboratory, University of California, Berkeley, CA, USA.

E-mail addresses: ronni@gi.alaska.edu (R. Grapenthin), jeff@gi.alaska.edu (J.T. Freymueller), sssu@emsd.ru (S.S. Serovetnikov).

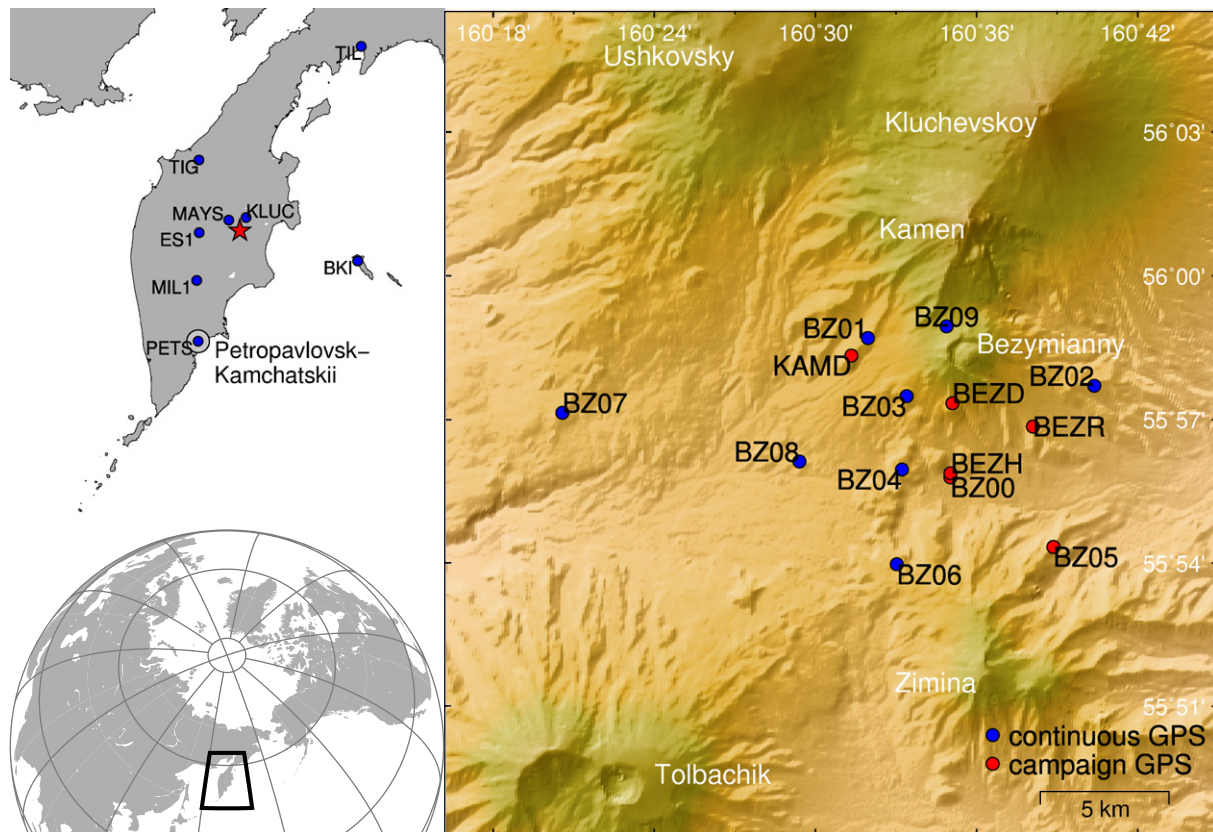


Fig. 1. Regional setting and available GPS data. World map (left bottom) outlines Kamchatka which is shown in the top left inset. Blue dots mark KAMNET continuous GPS stations. Red star marks location of the KGV. Right panel shows topographic map of the study region and location of PIRE GPS stations. Volcanoes are named in white text. Note the horseshoe-shaped crater with a new dome at Bezymianny. (For interpretation of the references to color in this figure legend, the reader is referred to the web version of this article.)

samples collected in 2007, 2009, and 2010 (López et al., *in press*) certainly strengthen the case of Thelen et al. (2010) for the existence of a very shallow reservoir. López et al. (*in press*) provide evidence for degassing of magma at shallow depths in August 2007 and July 2010; potentially within the edifice (pers. comm. with T. López, 2012). For July 2009, López et al. (*in press*) find evidence for the degassing of a deeper magma source, with the actual depth hard to constrain using current methods.

While long term seismicity from 1999 to 2010 draws a fairly clear picture supporting the subsurface structure described above (Thelen et al., 2010, their Fig. 1, or our Fig. 8), which is furthermore supported through petrologic studies (Turner et al., *this volume*), recent 4-D seismic tomography (Koulakov et al., *this volume*) suggests that the mid-crustal to shallow structures are more transient in nature and only the deep reservoir under Kluchevskoy appears permanent. This may be similar to interpretations of deformation at Kluchevskoy from 1981 to 88 by Fedotov et al. (1992) who interpret their observations with a migrating pressure source.

Until now this complex region has not been the target of dense GPS deformation studies. The last published geodetic study by Fedotov et al. (1992) gives an overview of leveling and triangulation surveys that were conducted from 1978 to 1989. Along one leveling line that runs east–west at about 3–4 km south of Bezymianny, Fedotov et al. (1992) report 45 mm of subsidence from 1978 to 1987 over a broad region (approx. 50–60 km). The source of this signal remains uninterpreted. Analysis of satellite data from 1992 to 2003 by Pritchard and Simons (2004a) reveals high rates of subsidence in the vicinity of the 1975–76 Tolbachik lava flows. No deformation due to any of the eruptions at the KGV volcanoes during that period could be resolved due to poor spatial and temporal coverage, which limits detection to larger signals in that region (Pritchard and Simons, 2004a).

Here, we present the first detailed geodetic study of the Bezymianny Volcano based on continuous and campaign GPS measurements spanning the years 2005–2010. This work is part of the Partnerships in International Research and Education program (PIRE-Kamchatka), sponsored by the National Science Foundation and carried out in collaboration with the Institute of Volcanology and Seismology (IVS) and the Kamchatkan Branch of Geophysical Services (KBGS). This project targeted the Bezymianny Volcano from a range of different perspectives (including Seismology, Petrology, Geodesy, Gas, Geology, Remote Sensing) to investigate the effect of sector collapse on the evolution of a volcanic system. Our main goals were (1) to explain the constant, network-wide subsidence observed during the investigation period, and (2) to investigate GPS time series for deformation related to individual explosive events and infer constraints for the subsurface magmatic system. To find answers to (1), we test various hypotheses including effects of subduction related strain accumulation, effects of surface load changes due to lava deposition and edifice growth, deflation of a deep magma reservoir replenishing the shallower reservoirs that drive the regular eruptions at Kluchevskoy and Bezymianny volcanoes, as well as combinations of those factors.

2. GPS data

2.1. GPS network

The geodetic network at Bezymianny consists of 8 continuous and 6 campaign sites (Fig. 1, Table 1); all were newly installed during the PIRE-Kamchatka project beginning in 2005. The network is intended for volcano deformation studies and thus provides good station coverage in both the near and the far field of the Bezymianny Volcano. Additional stations were planned to the north of Bezymianny to

Table 1
GPS benchmark coordinates and distance to Bezymianny dome (km). Installation dates (YYYY-MM-DD) represent the earliest available data.

4 Char ID	Lat (deg.)	Lon (deg.)	Height (m)	Installation date	Dist to dome (km)
BZ01	55.978378766	160.532566173	1998.7248	2006-10-06	4.0
BZ02	55.961769862	160.673119636	1615.8073	2006-10-07	4.9
BZ03	55.958141956	160.556598524	2071.6602	2006-10-06	2.9
BZ04	55.932567396	160.553716182	1671.3209	2006-10-07	5.2
BZ06	55.899598371	160.550529969	1715.9349	2006-10-06	8.6
BZ07	55.952326878	160.342916616	1497.2751	2007-12-02	16.0
BZ08	55.935400821	160.490028596	1472.6256	2007-12-02	7.8
BZ09	55.982467292	160.581416553	2539.8216	2006-10-06	1.5
<i>Campaign sites</i>					
BZ00	55.929872528	160.583754368	1445.8390	2007-07-21	4.8
BZ05	55.905622204	160.647691459	1552.9871	2007-07-21	8.1
BEZD	55.955679465	160.585075053	2126.5224	2005-08-22	2.0
BEZH	55.931323342	160.583882621	1453.8664	2005-08-21	4.6
BEZR	55.947547441	160.635012429	1638.5601	2005-08-22	3.6
KAMD	55.972258678	160.522331589	2016.3626	2005-08-21	4.6
<i>KAMNET sites</i>					
ES1	55.930500238	158.696605889	518.4864	1996-08-18	119.0
KLU	56.318416679	160.856016453	66.9442	1996-07-27	41.8
KLUC	56.318435566	160.856032316	66.8695	2008-08-27	41.8
MAYS	56.254257608	160.061819412	57.7978	2007-07-21	45.6
PETS	53.023299659	158.650134443	102.0694	1998-11-07	≈360.0

discriminate local deformation from the activity at Kluchevskoy Volcano. However, logistical constraints made it impossible to implement this part of the network.

The continuous sites are equipped with concrete pylons topped with SCIGN antenna mounts (Fig. 2A,C). The pylons were anchored in rock where available, but in most cases were anchored in soil more than 1.7 m below the surface. The exception was BZ09, which featured a smaller mount directly into the rock. Steel enclosures at the sites housed the receiver and batteries. Data were downloaded during annual service visits, during which we also changed batteries at the sites. Most of the campaign benchmarks are steel pins cemented in stable rock (Fig. 2B) and were first measured in 2005. Originally, the campaign sites BZ00 and BZ05 were intended for continuous observations and were built in the same fashion as the continuous sites. Logistical problems and/or concern of vandalism, however, prevented the permanent installation of receivers at these sites and they were measured annually during field campaigns together with the other campaign sites.

The continuous sites, and BZ00 and BZ05, have their earliest measurements in the summer months of 2006. Some stations suffer from significant data gaps (Fig. 3) due to power failures and animal damage (bear attacks). Since 2009 the sites BZ01, BZ03, BZ04, and BZ06 have been converted to solar powered operation. While the sites were intended to run only throughout the time of the project, this conversion made long-term operation through KBGS and IVS feasible.

In addition to the data from the Bezymianny network, KBGS provided data from their regional KAMNET network (Fig. 1, upper left inset). We use these data to get a sense for far field background velocities. ES1 is used as a reference station. Other stations do not qualify for such use as they are affected by inexplicable offsets (MIL1, likely an antenna change) or offsets due to earthquakes (TIG). The station KLU in the village of Kluchi was operated until 26 October 2008 when the benchmark was destroyed during construction. A new station (KLUC) was installed on 27 October 2008. KLUC shows similar long term trends as KLU. However, due to a lack of overlap of observations at KLU and KLUC we do not combine the data and for velocity estimates we refer to the data from KLU only.

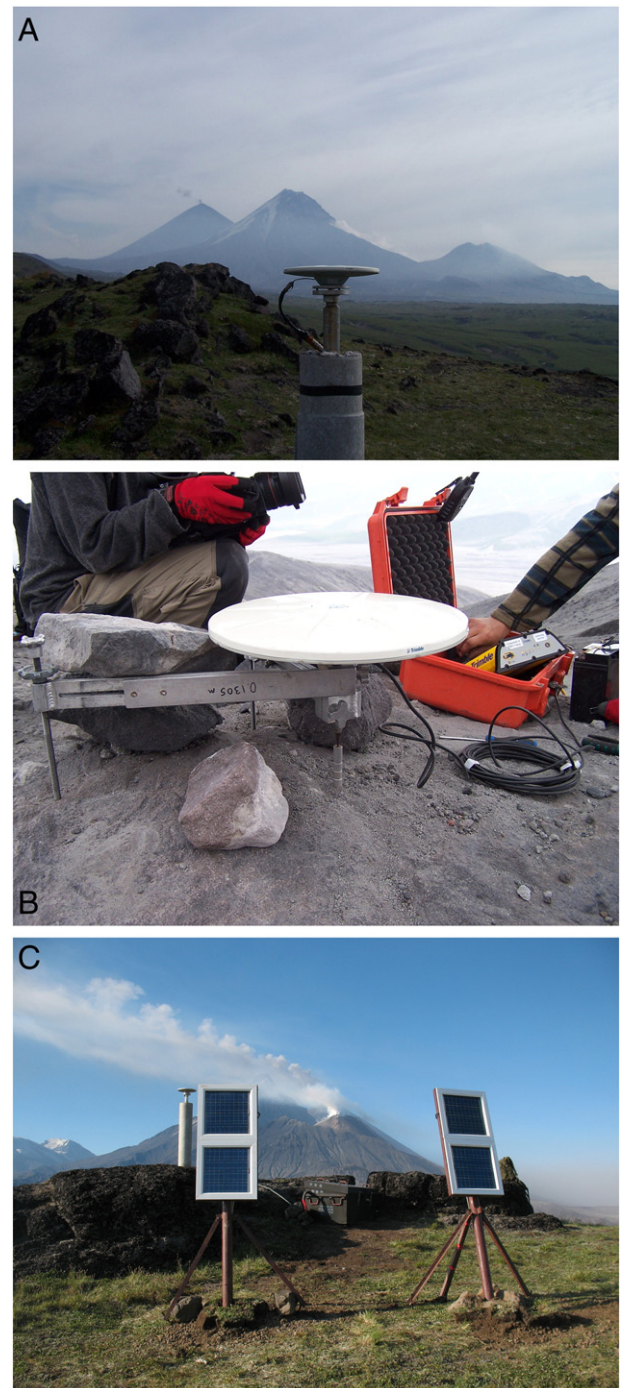


Fig. 2. (A) Continuous site BZ08 in summer of 2010. In the background: Kluchevskoy volcano with a small ash plume to the left, Kamen in the middle, and Bezymianny to the right and degassing. (B) Campaign site BEZR with spike mount setup and Trimble NetRS receiver in 2010. (C) Continuous site BZ06 with solar setup installed in 2010. The antenna is mounted on a concrete pylon, batteries and receiver are housed in the protective enclosure in the center, 4 solar panels were installed on 2 well anchored masts to keep them in place during high winds in that area. Bezymianny's dome steams in the background, which is the normal state.

2.2. GPS data processing

We use the GIPSY/OASIS II software (Gregorius, 1996) developed at NASA's Jet Propulsion Laboratory (JPL) to compute Precise Point Positioning solutions (Zumberge et al., 1997) for the GPS data. We analyze the GPS data together with the data from all available continuous and campaign GPS sites in north-west North America and north-

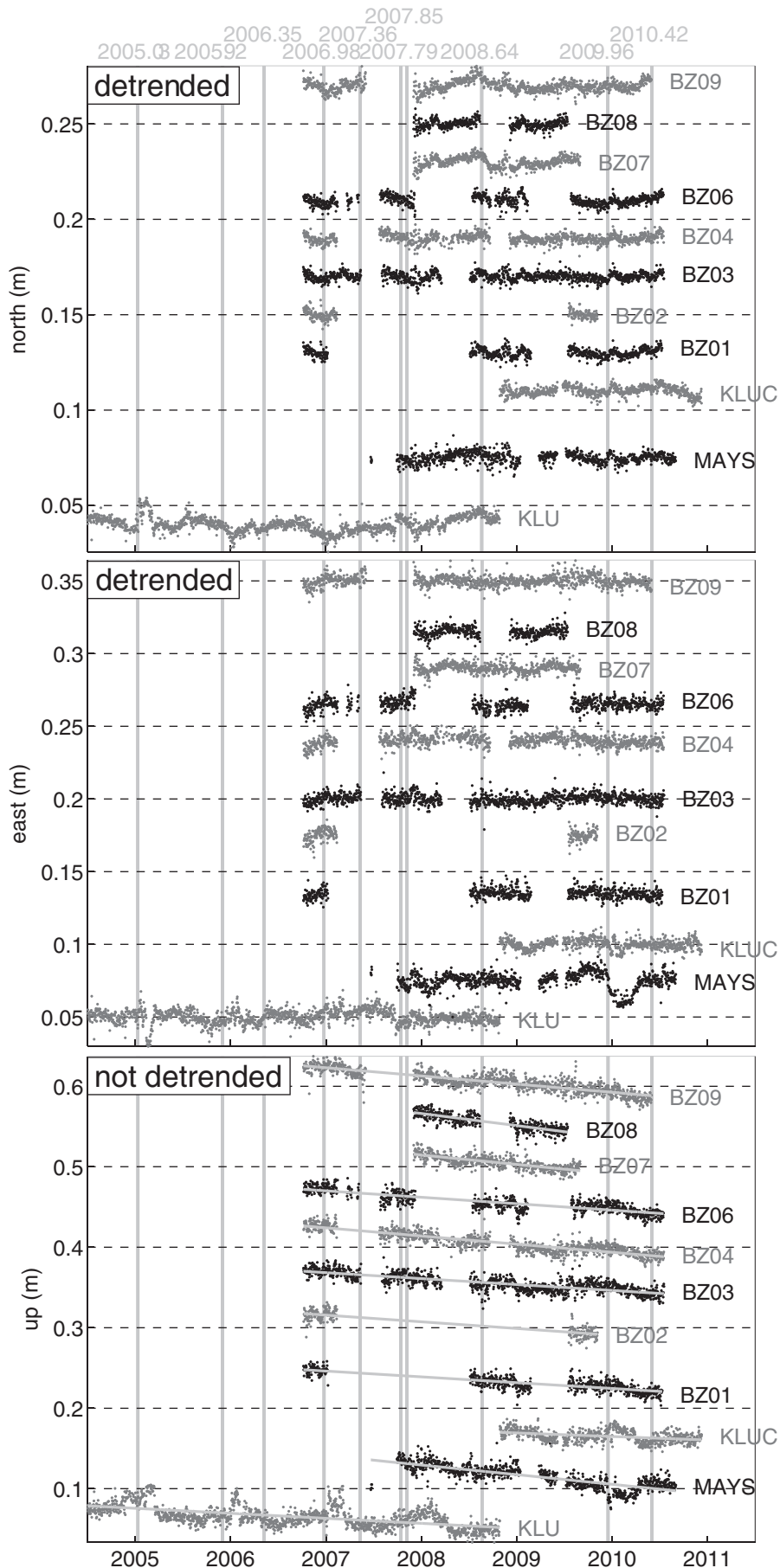


Table 2
Velocities (mm/yr).

4 Char ID	Wrt EURA (Fig. 4A)			Tectonics and ES1 removed ^a (Fig. 4B)			Load wrt ES1 removed ^b		
	N	E	U	N	E	U	N	E	U
BZ01	1.2±0.4	-10.4±0.3	-7.4±0.9	-3.7±0.6	1.0±0.6	-5.6±1.5	-3.8±0.6	1.2±0.6	-3.5±1.5
BZ02	2.0±0.4	-9.1±0.6	-8.1±1.3	-3.2±0.6	2.6±0.8	-6.3±1.9	-3.2±0.6	2.7±0.8	-4.3±1.9
BZ03	3.0±0.3	-8.7±0.3	-7.5±0.8	-2.1±0.5	2.8±0.6	-5.7±1.4	-2.0±0.5	3.0±0.6	-3.6±1.4
BZ04	2.4±0.3	-13.1±0.4	-10.2±0.7	-2.6±0.5	-1.5±0.7	-8.4±1.3	-2.6±0.5	-1.4±0.7	-6.4±1.3
BZ06	2.9±0.4	-10.8±0.5	-8.3±1.0	-2.2±0.6	0.9±0.8	-6.5±1.5	-2.2±0.6	1.0±0.8	-4.7±1.5
BZ07	0.1±1.3	-9.1±0.9	-12.0±1.7	-4.7±1.5	2.1±1.1	-10.2±2.2	-4.7±1.5	2.2±1.1	-8.4±2.2
BZ08	6.3±0.8	-5.5±0.9	-15.0±1.7	1.3±1.0	6.0±1.2	-13.2±2.3	1.3±1.0	6.1±1.2	-11.3±2.3
BZ09	1.4±0.5	-8.9±0.4	-10.2±0.9	-3.6±0.7	2.5±0.7	-8.4±1.5	-3.8±0.7	2.8±0.7	-5.7±1.5
<i>Campaign sites</i>									
BZ00	3.2±0.3	-12.1±0.9	-8.8±0.7	-1.9±0.6	-0.4±1.2	-7.0±1.2	-1.9±0.6	-0.2±1.2	-5.0±1.2
BZ05	5.7±0.5	-10.2±0.7	-7.6±2.8	0.4±0.7	1.6±1.0	-5.8±3.3	0.4±0.7	1.8±1.0	-4.0±3.3
BEZD	2.8±0.5	-8.4±0.8	-5.5±1.4	-2.3±0.7	3.2±1.0	-3.7±1.9	-2.2±0.7	3.3±1.0	-1.5±1.9
BEZH ^c	3.0±0.8	-12.1±0.5	-3.8±4.3	-2.1±1.0	-0.4±0.8	-2.0±4.8	-2.1±1.0	-0.2±0.8	-0.0±4.8
BEZR	7.9±0.7	-13.2±0.5	-12.0±1.3	2.7±1.0	-1.5±0.8	-10.2±1.9	2.7±1.0	-1.4±0.8	-8.2±1.9
KAMD	2.6±0.5	-8.3±0.9	-4.6±1.2	-2.4±0.7	3.1±1.2	-2.8±1.7	-2.4±0.7	3.2±1.2	-0.8±1.7
<i>KAMNET sites</i>									
ES1	4.1±0.2	-9.8±0.3	-2.1±0.6	0	0	0	0	0	0
KLU	4.3±0.7	-9.6±0.8	-4.2±3.0	-0.4±0.9	1.2±1.1	-2.3±3.5	-0.2±0.9	1.4±1.1	-1.5±3.5
MAYS	2.7±0.5	-6.7±1.3	-5.3±2.2	-1.5±0.7	3.5±1.6	-3.2±2.8	-1.4±0.7	3.5±1.6	-2.4±2.8
PETS	12.0±0.3	-24.7±0.4	-5.2±0.6	6.9±0.5	-8.6±0.6	-5.5±1.1		n/a	

^a ES1 predicted subduction velocities (mm/yr): E = -2.5, N = 2.8, U = 0.4.

^b ES1 predicted load velocities (mm/yr): E = 0.1, N = 0.0, U = -0.4 (see Table 4).

^c BEZH shows strong variation in the vertical for measurements in 2005 and 2006 which results in a lowered long term subsidence. As BZ00 is very close, we ignore measurements at BEZH.

east Asia to generate time series of daily positions (Fig. 3). Details on parameter estimation are given in Freymueller et al. (2008) and Freymueller and Kaufman (2010). Our data analysis strategy is described in Fu and Freymueller (2012). To estimate station velocities and their uncertainties assuming a power-law noise model, we use the time series analysis software CATS (Williams, 2008) and give results relative to stable Eurasia as defined by Argus et al. (2010) (Table 2, Fig. 4A).

We also estimated station positions for BZ09 kinematically at each epoch (30 s intervals) using BZ06 or BZ03 as base station and processed the data similar to Grapenthin et al. (in press-a). However, the resulting time series show no significant explosion related deformation above background noise so we will not report further details on this work.

2.3. Time series observations

The main and most perplexing observation from the time series is that a region greater than 50 km in radius, encompassing the entire KGV, is subsiding rapidly. Fig. 3 illustrates this in the vertical position time series for the continuous sites. All sites in the Bezymianny network subsided rapidly over the entire study period at relatively uniform rates between about 8 and 12 mm/yr (Table 2). The campaign sites BEZD and KAMD subside at less than 7 mm/yr and the continuous site BZ08, built on a mound of softer soil, subsides at 15 mm/yr. Note that we ignore BEZH due to inconsistent measurements in the vertical component for 2005 and 2006 compared to the rest of the campaign results and its close proximity to BZ00, which shows position changes more consistent with the rest of the network.

The KAMNET sites in Kluchi (KLU/KLUC, about 42 km to the NNE) and Mayskoe (MAYS, about 45 km to the NW) show similar but slightly slower subsidence at respective rates of 4.3 and 5.3 mm/yr.

Even the more distant KAMNET site in Esso (ES1, about 120 km to the E) subsides at about 2.1 mm/yr. The spatial variations of these subsidence rates do not show an obvious relationship in the position of the sites relative to the Bezymianny Volcano but indicate that the main signal source is limited to the KGV. Pinpointing this down to a simple, small scale signal source is difficult as the rate of relative horizontal motion is small (Table 2).

The second – equally perplexing – observation from the time series is that most of the GPS sites do not show variations in their horizontal or vertical motions that correlate with the times of the eruptions (Fig. 3, eruptions are marked by vertical gray lines). An exception is the late 2006 eruption, which induced a small signal at several sites (Fig. 3). The time series prior to the event, however, are too short to make a definitive statement given the small signal amplitude.

The site BZ09, located only 1.5 km from Bezymianny's dome, does show small variations in motion that correlate with the eruptions at 2007.36, 2008.64, and 2010.42 (times are given in decimal years). In the months before an eruption, the site shows a tendency to move northward at a rate faster than average, and then move southward again at the time of the eruption. This pattern would be expected from the pressurization and depressurization of a magma source located near the summit of the dome. However, the variations (approx. 1 cm) are close to the level of noise.

Two additional stations show motion that deviates from average trends at times of eruptions. BZ07 moves rapidly south during and after the eruption in 2008.64 and then continues to follow the pre-eruptive trend. Since BZ08, the nearest site to BZ07, is not operational during this time and no other station of the network shows similar motion, we assume that this motion was very local and coincided with the eruption rather than being triggered by the event. MAYS shows a very interesting pattern of slight eastward motion prior to

Fig. 3. Time series of continuous GPS stations from 2005 to 2011 in the KGV. The north and east components have been detrended (see Fig. 4 for the velocities), while the vertical time series has not, and is shown in ITRF2008. Vertical gray lines indicate eruptions of Bezymianny. Times for individual eruptions are given in decimal years above the top panel. The removed long-term trends in the north and east component are mostly due to motion of the Okhotsk plate and subduction of the Pacific plate to the east. Note the network wide subsidence in the vertical component. BZ09 deviates slightly from the long term trend around eruption times in the north component. BZ07 shows curious motion in the north component during and shortly after eruption 2008.64; likely not related to the eruptive activity. MAYS moves prior to and following the 2009.96 event, but it remains speculation whether the eruption actually induced motion at MAYS since KLUC does not show significant motion during this time period although it is an equal distance from the volcano.

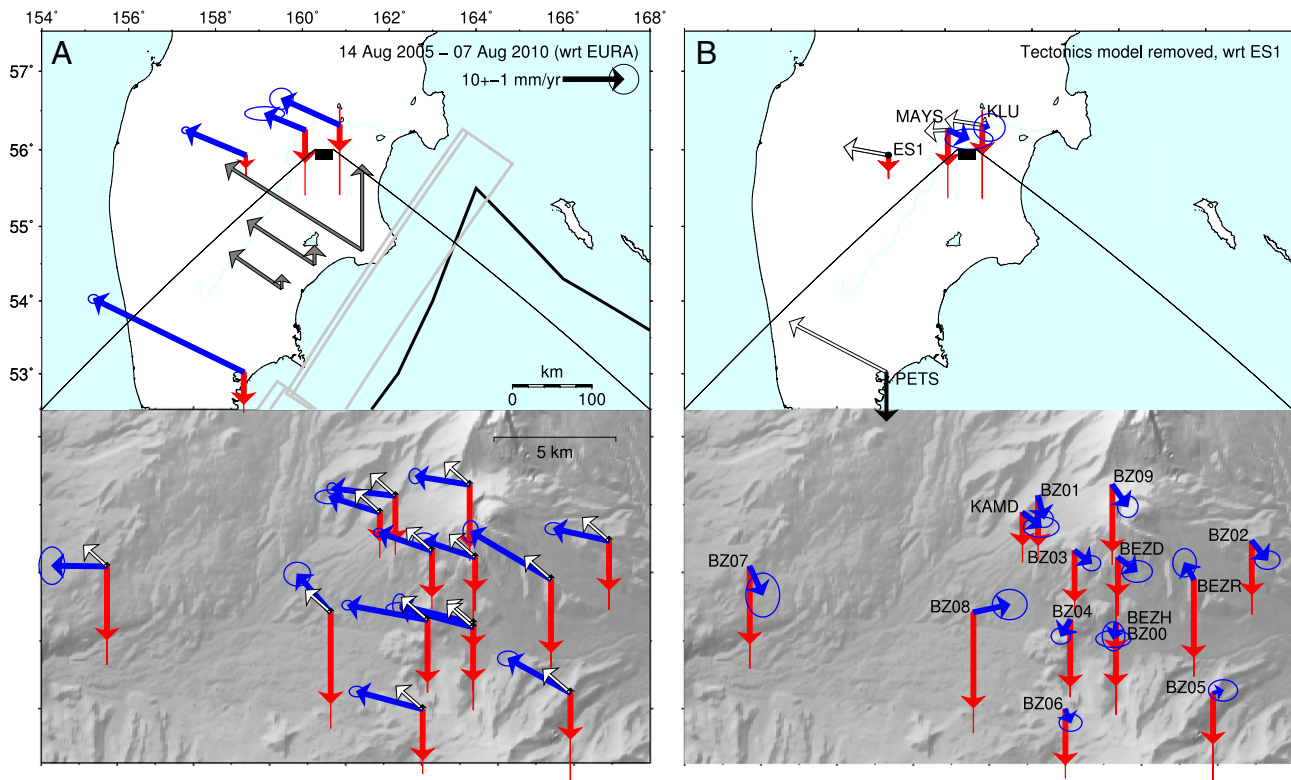


Fig. 4. Velocities inferred from 2005 to 2010 time series for central Kamchatka and Bezymianny Volcano. (A) Colored vectors (blue: horizontal, red vertical) show site velocity calculated from 14 Aug 2005–07 Aug 2010 relative to stable Eurasia (Argus et al., 2010). Arrows are tipped with associated uncertainties given at the 95% level. Gray vectors show tectonic motion of overriding plate due to subduction of the Pacific plate based on the model of Bürgmann et al. (2005, Table 2, model 5a and 5b) for hypothetical stations, which illustrates the decay of deformation with distance from the trench. Their 2 plate model is outlined in gray, next to an approximation of the surface expression of the trench (black). Inset shows data for the Bezymianny region. White and black vectors are the tectonic model predictions. Note that vertical predicted motion due to tectonics is plotted but negligible at this distance from the trench. (B) White and black vectors are residuals of data minus model given in Panel A. Colored vectors station velocities with respect to stable ES1. Note that these values are only given for stations whose velocities are to be modeled later (PETS excluded). Data relative to ES1 show clear network wide subsidence extending northwards to KLU and westwards to MAYS. Horizontal velocities seem highly uncorrelated in the Bezymianny network. (For interpretation of the references to color in this figure legend, the reader is referred to the web version of this article.)

the 2009.96 eruption. During and after the event the site moves first west, then back east, and finally re-assumes the prior long-term trend with no visible static offset. If this signal was volcanic in origin, it would indicate deep deflation prior to the 2009.96 event and then immediate recharge of this deep pressure source. This interpretation remains a speculation since station KLUC at a similar distance to the KGV does not show significant deformation during this time period (displacement at KLUC would be expected in the north component for most volcanic sources, Fig. 3).

3. Long-term, long-wavelength subsidence

In this section we investigate the main sources that could induce regional subsidence on the scale we observe at Bezymianny: strain accumulation at a subduction zone, loading deformation due to deposition of volcanic products and deformation due to a volcanic source. None of these processes are particularly well understood in this region, subduction strain accumulation certainly being the best measured and modeled based on GPS data (Bürgmann et al., 2005). However, first order approximations based on conservative model parameter definitions will allow us to identify which of these processes dominates and gives the best explanation of the observations.

3.1. Tectonic displacements

Tectonically, Kamchatka is part of the Okhotsk micro plate (Apel et al., 2006). While the exact motion of this plate is somewhat controversial and poorly constrained (e.g., Shestakov et al., 2011), Kamchatka

clearly moves independently from the North American and Eurasian plates. In addition to the resulting rotational component, the Pacific plate subducts beneath Kamchatka at a rate of ≈ 80 mm/yr (e.g., Bürgmann et al., 2005) which induces active deformation south of the intersection with the Aleutian trench ($< 56^\circ$ N). Vertical motions are expected from such strain accumulation at subduction zones (Savage, 1983). Inverting interseismic GPS data, Bürgmann et al. (2005) proposed models for the plate interface of the subduction zone and the related slip along these fault models. We apply these models and select one (model 5) to eliminate interseismic strain that accumulates over the time of our observations. Fig. 4A shows in colored vectors the site velocities (blue: horizontal, red: vertical) inferred from time series spanning 2005 to 2010 (KLU: 2005–2008) with respect to stable Eurasia (Argus et al., 2010). The white and black vectors in the same figure show velocities of the overriding plate induced by the underthrusting Pacific plate as proposed by Bürgmann et al. (2005, Table 2 model 5). This two-fault model is outlined in gray in Fig. 4A. Although fully modeled, only a small part of the southern plate interface model is visible in the figure. We clearly see a reduction in the predicted horizontal velocity with increasing distance from the trench (Fig. 4A white). The relative motion between the Bezymianny network and ES1 is about 2–3 mm/yr. Without removing the model from the velocities this bias would be introduced in the horizontal velocities of the Bezymianny network once we use any of the more distant sites as a reference station. More importantly, however, the predicted vertical motion at the Bezymianny network is virtually zero and hence does not explain any of the subsidence we observe. Slight subduction related modeled uplift is plotted as black

vectors in Fig. 4A. Nevertheless we use this model to correct for interseismic velocities.

Subtracting the predicted subduction zone velocities from the velocities with respect to stable Eurasia gives the white and black vectors in Fig. 4B. This approximates the motion of the Okhotsk plate relative to stable Eurasia. To eliminate this component, we subtract the residual motion at ES1 (vectors in Fig. 4B) from the Bezymianny network including stations MAYS and KLU. The results are the colored vectors in Fig. 4B which we only show for MAYS and KLU as the other sites are not relevant for our study. The plotted uncertainties are propagated from the original uncertainties shown in Fig. 4A with the horizontal uncertainties for ES1 added in quadrature. Note that the vertical motion at ES1 is not removed in Fig. 4B to visually stress, again, the extent of the subsidence that persists after tectonic correction (5–15 mm/yr, Table 2). The directionality of the residual horizontal velocities (up to 6 mm/yr, Table 2) does not suggest an obvious single signal source and may be a combination of rotational difference between ES1 and the Bezymianny network (likely small, and systematic across the network) and an unmodeled tectonic component.

3.2. Surface load models

To understand the cause of the rapid network wide subsidence observed for the Bezymianny network and to avoid biases in the estimation of a volcanic source (Grapenthin et al., 2010), we test whether destruction of the pre-1956 edifice, the rapid rebuilding of Bezymianny's dome, and the reoccurring pyroclastic flow deposits since then could induce displacement rates large enough to explain the observations. We include the impact of the ongoing rapid build-up of the Kluchevskoy Volcano and the 2.2 km³ of material erupted during the 1975 Tolbachik fissure eruption (Fedotov and Markhinin, 1983; Fedotov et al., 2010).

To model the response of the crust to changes in surface load, we model the Earth as a half-space of Newtonian viscosity overlain by an elastic plate. Recent displacement rates are estimated from Green's function derived by Pinel et al. (2007; Equation A3), which are implemented in the framework CrusDe (Grapenthin, 2007) used for

our simulations. For simplicity, we approximate all loads as (combinations of) disk loads (Fig. 5). Individual disk heights are determined by volume redistribution based on the geometric shape of the feature, e.g., the Bezymianny dome is approximated by a half sphere, and the Kluchevskoy Volcano by a cone (see Table 3 for all load values). The density of each load is assumed to be 2600 kg/m³.

The growth rate for the Kluchevskoy Volcano was inferred by calculating the volume for a cone starting at 1400 m asl with a base radius of 7 km and a height of 3400 m. When we divide the resulting total volume by the 7000 years of eruptive activity, we get a growth rate of 0.0245 km³/yr. This is very similar to a rate of 0.0231 km³/yr that can be inferred from the annual mass output of the Kluchevskoy Volcano given by Fedotov et al. (2010, assuming a density of 2600 kg/m³ for basalt).

We have to make several assumptions on crustal properties. We assume a 30 km effective elastic plate thickness (considering the assumption of a large magma body below that depth), an effective Young's modulus of $E = 80$ GPa, and a Poisson's ratio of 0.25. The mantle is assumed to have a density of $\rho_m = 3100$ kg m⁻³ (e.g., Pinel et al., 2007) and a viscosity of $\eta = 4 \times 10^{19}$ Pa s (Turcotte and Schubert, 2002).

These parameter values result in a visco-elastic relaxation time $\tau_{ve} = 2\eta/E \approx 32$ yr (Turcotte and Schubert, 2002). Given the short wavelength of the loads (<30 km) compared to the assumed elastic thickness (30 km), we can neglect any viscous effects from deeper in the mantle. This effect must be taken into account if compensation of the load due to the build-up of the entire KGV was modeled. While this may contribute significant deformation, the long-term load history is too poorly constrained to create a realistic model.

Due to their greater distance from the GPS stations, we estimate current displacement rates induced by the 1975–76 Tolbachik products and activity at the Kluchevskoy Volcano on a 1 × 1 km grid (Fig. 5, map box limits model region). To reach a steady state velocity for the ongoing build-up of the Kluchevskoy Volcano, we run this simulation over the last 200 years. The Tolbachik loads are added at model time step 165 (real-time year 1975). The velocities at grid nodes closest to station coordinates at model time 200 are the estimated velocities for the year 2010. The velocities induced by Bezymianny products are

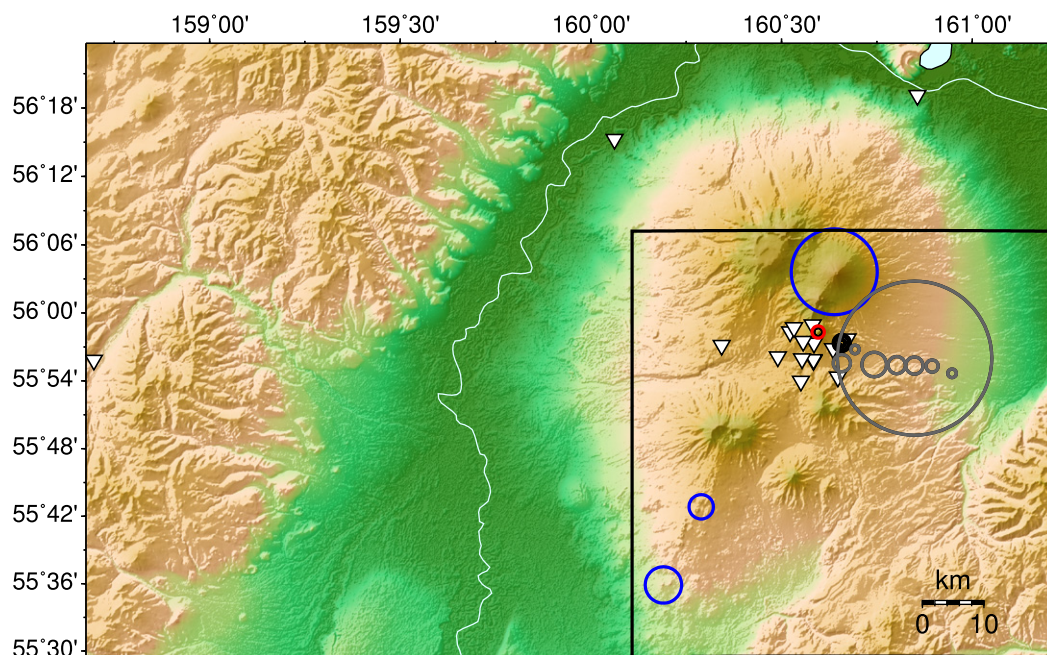


Fig. 5. Spatial distribution of disks used to estimate velocities due to changes in surface loads listed in Table 4. Precise definitions of the disk values are given in Table 3. The map boundary corresponds to the area for which the Kluchevskoy and Tolbachik loads (blue circles) were modeled on a 1 × 1 km grid. The black box outlines the area for which subsidence due to the Bezymianny loads (gray: 1956 deposits, red: 1956 edifice removal, black: post 1956 products) was modeled on a 0.5 × 0.5 km grid. (For interpretation of the references to color in this figure legend, the reader is referred to the web version of this article.)

Table 3
Loads used to estimate velocities listed in Table 4.

Load	Longitude	Latitude	Radius (km)	Height/growth rate	Source
Kluchevskoy edifice	160.63809394	56.06029411	7.0	0.16 m/yr	Fedotov et al. (2010), this study
Tolbachik 1975 North	160.28928123	55.71397898	2.0	95 m	Fedotov et al. (2010)
Tolbachik 1976 South	160.19025419	55.59815859	3.0	35 m	
<i>Bezymianny 1956</i>					
Edifice	160.59589619	55.97188339	1.0	–159.2 m	Belousov et al. (2007)
Ash deposits	160.84885332	55.93329979	12.6	0.39 m	
Debris flows	160.65803826	55.92613096	1.4	11.59 m	
	160.69253144	55.94633073	0.7	23.19 m	
	160.74277732	55.92406240	2.0	8.52 m	
	160.80195775	55.92321073	1.4	17.39 m	
	160.84834015	55.92252335	1.4	17.39 m	
	160.89472051	55.92181851	1.0	11.36 m	
	160.94700033	55.91111735	0.7	23.19 m	
<i>Bezymianny pyroclastic flows, 2007 and younger</i>					
2007	160.65770426	55.95579068	1.1	4.47 m	Zharinov and Demyanchuk (2011)
2007			1.3	7.16 m	
2008			0.5	3.82 m	Girina (this volume)
2008			0.5	3.82 m	
2009			0.6	1.77 m	
2010			1.4	3.74 m	
<i>Bezymianny dome growth</i>					
1956–1967	160.59589619	55.97188339	0.75	13.52 m/yr	Zharinov and Demyanchuk (2011)
1967–1976				7.02 m/yr	
1983–1994				1.61 m/yr	
1994–2006 (–2010)				4.06 m/yr	

estimated separately on a 0.5×0.5 km grid (Fig. 5, black box indicates model region) and, since the method of Green's functions requires linear behavior, added to the results for Tolbachik and Kluchevskoy (see electronic Supplements 1,2).

The results of these simple experiments that assume a conservative Earth model indicate that loading cannot be neglected when we try to understand the displacement field at Bezymianny (Table 4). However, the maximum modeled load induced subsidence rate of 3.1 mm/yr at BZ09 is still small compared to the observed values. For the more distant sites KLU and MAYS the model still predicts 1.2 mm/yr of subsidence (ES1: 0.4 mm/yr) (Fig. 6); this is mainly due to Kluchevskoy's ongoing growth. With such small rates in the vertical field, displacement rates in the horizontal field are negligible

Table 4
Modeled site velocities induced by surface loads.

4 Char ID	East (mm/yr)	North (mm/yr)	Up (mm/yr)
BZ01	–0.1	0.0	–2.4
BZ02	0.0	0.0	–2.4
BZ03	–0.1	0.0	–2.4
BZ04	–0.1	0.0	–2.3
BZ06	–0.1	0.0	–2.2
BZ07	0.0	0.0	–2.1
BZ08	0.0	0.0	–2.3
BZ09	–0.1	0.2	–3.1
<i>Campaign stations</i>			
BZ00	–0.1	0.0	–2.3
BZ05	–0.1	0.0	–2.2
BEZD	–0.1	–0.1	–2.6
BEZH	–0.1	0.0	–2.4
BEZR	0.0	0.0	–2.4
KAMD	–0.1	0.0	–2.4
<i>KAMNET sites</i>			
ES1	0.1	0.0	–0.4
KLU	–0.1	–0.2	–1.2
MAYS	0.1	–0.2	–1.2

(fractions of mm/yr, see Table 4) and the surface load modeling, while inducing a complex deformation pattern, does not clarify the observed complex horizontal velocities at Bezymianny.

3.3. Volcanic sources

Having eliminated subduction and surface loading as main contributors to the observed subsidence rates at Bezymianny, we will now assess the likelihood of a volcanic source inducing such regional scale deformation as indicated by our observations. Deep volcanic inflation over similar-sized regions has been observed before in South America (Pritchard and Simons, 2004b; Fournier et al., 2010), which suggests that we may be observing a similar phenomenon.

Some tests with forward models using a deep pressure point source (Anderson, 1936; Yamakawa, 1955; Mogi, 1958) and an oblate spheroid (Yang et al., 1988; Battaglia et al., in press) yield good fits to the vertical deformation field, but significantly overestimate displacements in the horizontal field. A simple source that generates large vertical and small horizontal displacements is a sill, which we model as a closing tensile fault (Okada, 1992).

Effectively, it is possible to fit the observed subsidence with any sill in the lower crust that changes in volume by about the amounts estimated for the annual volume output of the KGV ($0.023\text{--}0.057$ km³/yr, converted to volumes from mass estimates given by Fedotov et al. (2010) assuming density of basalt). We attempted various kinds of source estimations/data inversions including grid searches (similar to (Grapenthin et al., in press-a)) and simulated annealing (e.g., Cervelli et al., 2001). In these procedures we evaluated model fits with respect to ES1 for a range of subsets of the data: (1) load model removed/not removed; (2) only stations >4 km away from Bezymianny; (3) including/excluding KLU, MAYS; and (4) using only vertical or full 3D velocities.

Except for a geometry preference towards a deep, large sill, rather than spherical sources, the results to these inversions remain inconclusive. In fact, Fig. 7 presents histograms from these experiments that indicate the spread of best fitting parameter sets. We ran 5000 experiments on each set of input data listed above (see caption of Fig. 7). The parameters for the sill were limited to a 40×40 km area

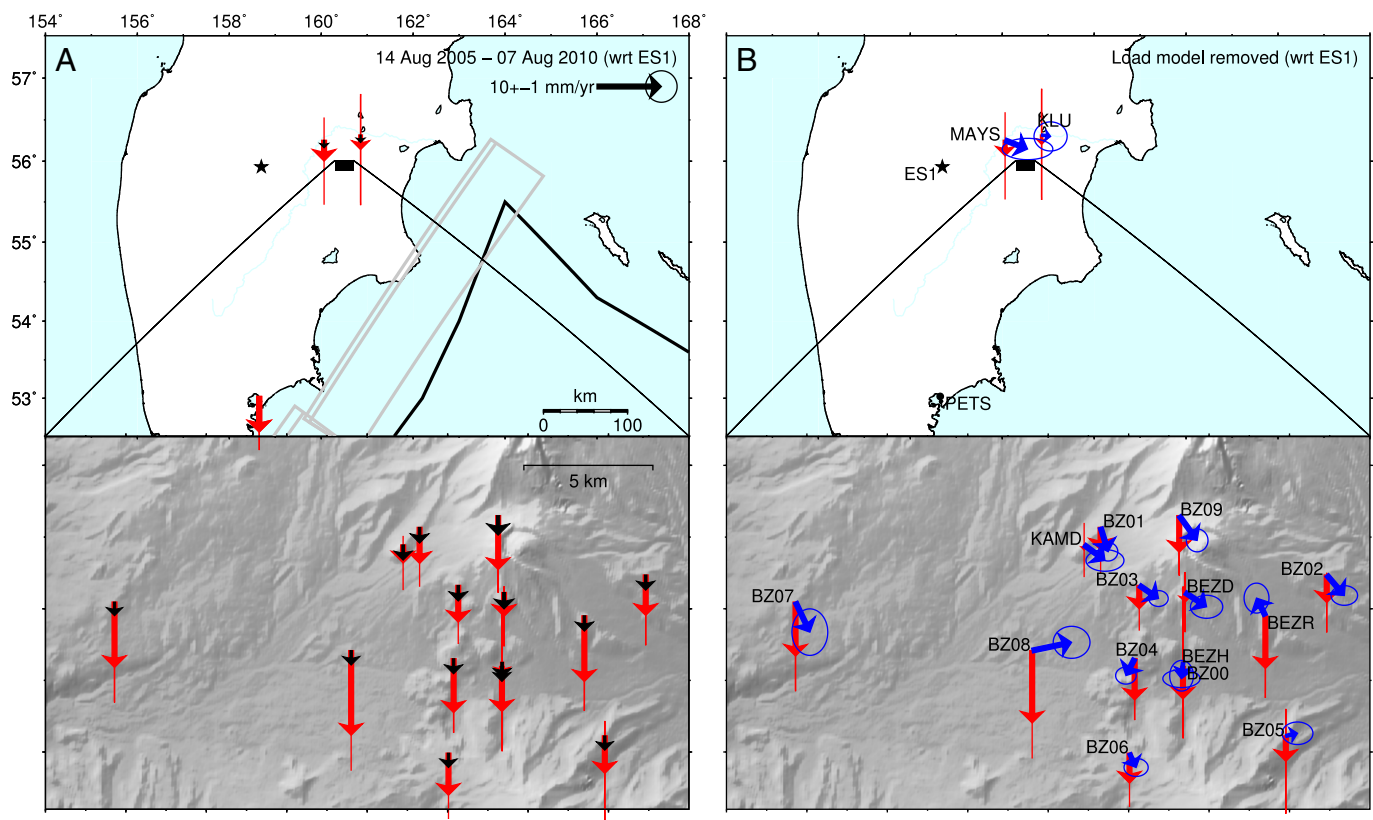


Fig. 6. Load velocity model results. (A) Measured vertical velocities with tectonics model removed and relative to ES1 (star). Black vectors are prediction of vertical velocities due to load model as defined in Fig. 5 (horizontals are negligible and not plotted for clarity, see Table 4). (B) Residual velocities after removal of load predictions (blue: horizontal, red: vertical). (For interpretation of the references to color in this figure legend, the reader is referred to the web version of this article.)

around the Bezymianny Volcano, depths from 1 to 50 km, lengths and widths from 1 to 40 km, opening from -10 to 0 m, strike from -180 to 180° , and dip from 0 to 90° . Best fits to the data can be found for any of these subsets. All of these tend to put the sill at rather large depth with its center of gravity roughly south and anywhere between east and west from Bezymianny. Misfits can be minimized either with a very small area sill (no impact on data) or a wide and long sill with small opening, striking roughly north–south and dipping at angles smaller than 20° .

This seems to contradict previous findings from seismology and seismic tomography. Fedotov et al. (2010, their Fig. 19) propose a complex plumbing system underneath the entire KGV with a deep source at about 30 km beneath the Kluchevskoy Volcano feeding into intermediate storage regions under Bezymianny and Kluchevskoy, respectively. Koulakov et al. (2011, this volume) find a robust deep velocity anomaly under Kluchevskoy, which they interpret as a pool of magma.

If the Fedotov et al. (2010) description of the plumbing system is accurate, our results imply that the pressures change very little with time in all of the shallow bodies, so that only the depressurization of the deep body induces significant deformation. As the KGV shows sustained high levels of volcanic activity, continuous withdrawal from a deep, common magma storage region seems plausible. Therefore, we test the hypothesis of deflation of a deep sill located underneath Kluchevskoy and constrain this model in accord with long-term seismicity (e.g., Fig. 8): (1) EW extent: 9.46 km; (2) NS extent: 12.75 km; (3) depth of fault plane: 33.5 km; (4) dip: 13° E; and (5) strike: 200° N.

The remaining unconstrained parameter is the opening for which we perform a grid search from -1 to 0 m in 0.001 m intervals. We determine that -0.22 m/yr (-0.16 m/yr when fitting the load corrected data) of opening fits the vertical displacements best. This results in an annual volume change of 0.027 km³ (0.019 km³/yr for

load corrected opening), which is a reasonable value compared to the productivity of 0.023 km³/yr of Kluchevskoy we derived above.

The predictions of this model (Fig. 9), along with the velocity field relative to ES1, are shown in Fig. 10A. The horizontal residuals in Fig. 10B suggest some remaining, southward motion of the entire network. Only the campaign site BEZR, a station on a ridge in the pyroclastic flow path, and the continuous site BZ08, the continuous station with fewest data (Fig. 3), do not conform with this overall trend. The coherence of the remaining horizontal residuals may indicate a small ≈ 5 – 7 mm/yr residual motion of the Bezymianny network relative to ES1 on the opposite side of the Central Kamchatka Depression. This residual motion is roughly trench-parallel, so it is likely not related to any shortcoming in the subduction strain model. However, it could represent a small shear motion across the Central Kamchatka Depression.

This gain in consistency in the horizontal component supports the assumption of long term deformation at Bezymianny being driven by the deep sill-like source under Kluchevskoy. Our solution is non-unique, however, considering the uncertainties in the velocities, the long wavelength and small amplitudes of deformation, our model seems to provide a reasonable and conservative explanation for the observations. Data spanning the entire KGV would be required to constrain a unique best-fitting model.

4. Short term displacements: individual eruptions

The daily positioning time series for continuous GPS stations around Bezymianny show no clear signal in either vertical or east component related to explosive events from 2005 to 2010 (Fig. 3). In the north component only BZ09 shows slight variations indicating northward motion prior to eruptions at 2006.98, 2007.36, 2008.64,

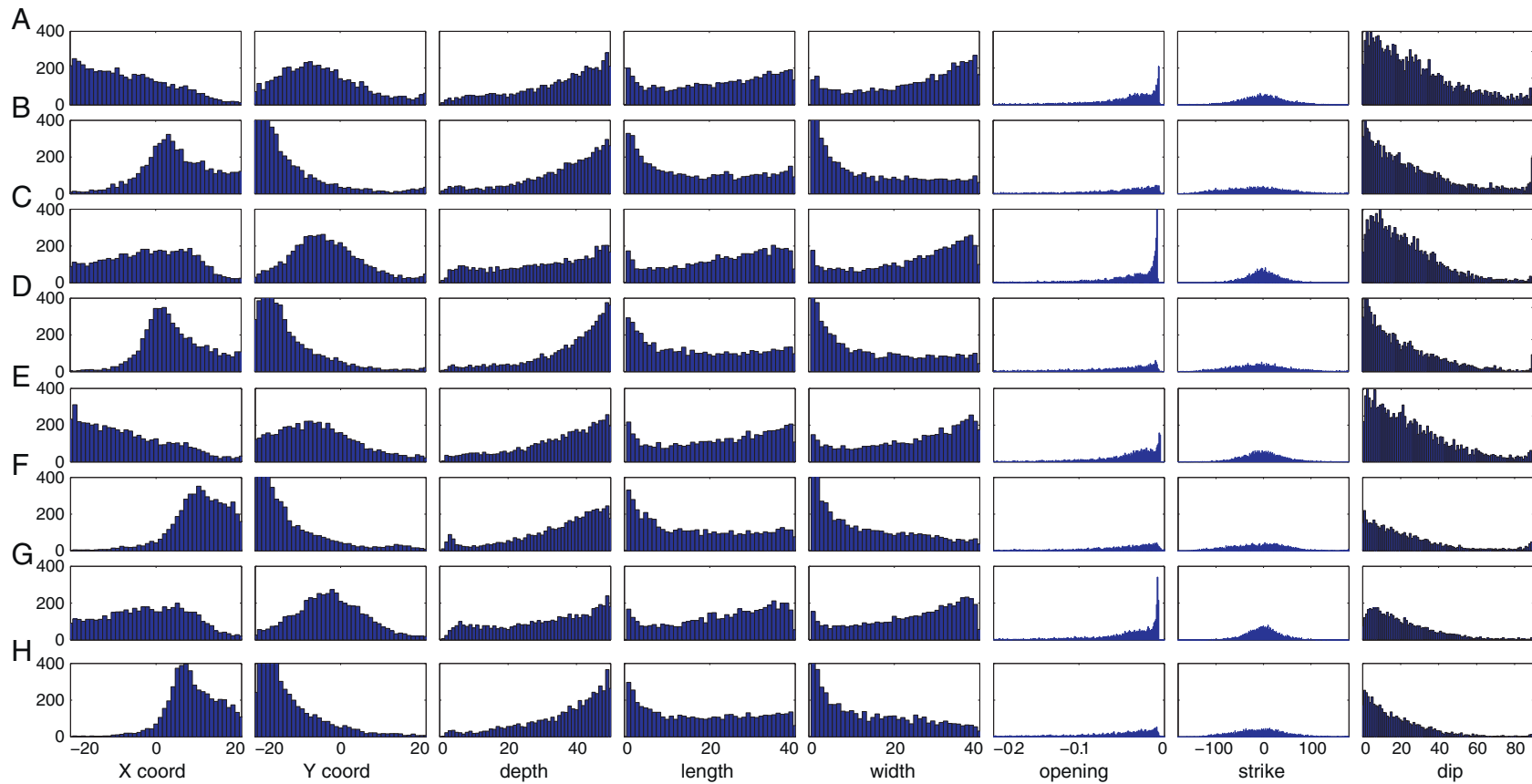


Fig. 7. Histograms showing the distribution of best fitting parameters from 5000 simulated annealing experiments each using different input data. (A) South Bezymianny stations and vertical displacements used for fitting, load correction applied. (B) South Bezymianny stations and 3-D displacements used for fitting, load correction applied. (C) South Bezymianny stations and vertical displacements used for fitting, no load correction applied. (D) South Bezymianny stations and 3-D displacements used for fitting, no load correction applied. (E) All stations and vertical displacements used for fitting, load correction. (F) All stations and 3-D displacements used for fitting, load correction. (G) All stations and vertical displacements used for fitting, no load correction. (H) All stations and vertical displacements used for fitting, load correction applied.

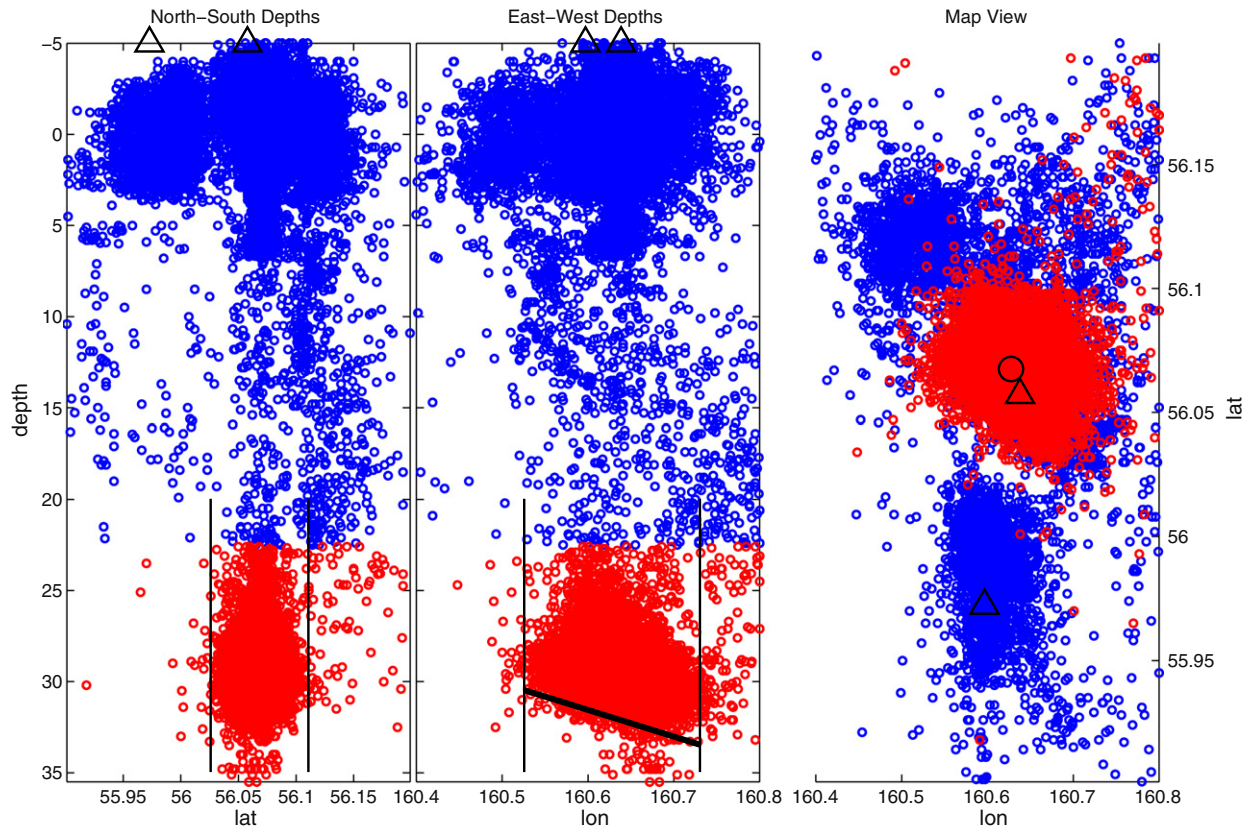


Fig. 8. Seismicity under the KGV (KBGS catalog, 1999–2010). Left: North–south section through the group and projection of earthquakes to a depth of 35 km onto one plane; earthquakes below 22 km are marked red. Triangles mark locations of Bezymianny (left) and Kluchevskoy (right). Several clusters of seismicity emerge. Black vertical lines mark the limits of the width of the sill we use in the forward model. Middle East–west section. Bezymianny is right triangle, Kluchevskoy is the left one. Black vertical lines mark the limits of the length of the sill we use in the forward model. The tilted gray line emphasizes an apparent dip in the bottom limit of seismicity. The dip of this line is about 13° , which is used in our sill model. The deep end of this line is at 33.5 km, which constrains the depth of our sill. Right: Map view of the seismicity. Triangles mark Kluchevskoy (north) and Bezymianny (south). Seismicity below 22.5 km is again colored red and clearly clusters under Kluchevskoy. The center point of the model sill is marked by the circle. (For interpretation of the references to color in this figure legend, the reader is referred to the web version of this article.)

2010.42 and southward motions following these events (if the antenna was not destroyed by ballistics as was the case during the 2010.42 event) and likely also at 2009.96. This means all events for which we have data at this location appear to induce subtle motion in the site's north component. While this motion stands out above background, it is too small to infer eruption related offsets that would enable source modeling. Even if we could do this and dealt with large uncertainties, the resulting single observable is not sufficient to derive a unique source. Instead, we follow Grapenthin et al. (in press-a) in their approach of analyzing the sensitivity of a GPS network to test likely source locations for their detectability. This limits the seemingly infinite parameter space to a more informative range.

For reservoirs located under Bezymianny several depths have been previously proposed (e.g., Fedotov et al., 2010; Thelen et al., 2010; Koulakov et al., 2011). However, no source geometries were inferred so we assume the most simplistic model under Bezymianny's summit: a pressure point source, or Mogi source (Anderson, 1936; Yamakawa, 1955; Mogi, 1958). In addition to a horizontal location (which we constrain) this simple analytical model requires only source depth and volume change to provide surface displacements.

At fixed horizontal locations – one directly under the summit, the other one in the blast zone about 2 km to the south-east of Bezymianny (West, this volume) – we vary the source depth and at each depth level we search for the minimum volume change required to induce ≥ 1 cm of horizontal or vertical displacement. Doing this for each station produces the colored contours in Fig. 11. The blue-shaded region in Fig. 11A,B indicates depth–volume change combinations that induce

at least 1 cm horizontal or vertical displacement at a minimum of one station, which we can reject based on the lack of deformation observed. White areas of the plot indicate depth–dV combinations that would produce deformation too small to observe, and we can neither confirm nor reject any such model. Previous work proposed sources at shallow levels (1 km, 7 km (Thelen et al., 2010)), mid-crustal levels (10 km, 18 km (Fedotov et al., 2010)), and at the base of the crust (25–30 km (Fedotov et al., 2010; Koulakov et al., 2011)), which we mark with the horizontal dashed gray lines in Fig. 11.

In addition to these proposed source depths, we can plot ranges for estimated volume changes. The lava flows from 1984 to 2007 (Zharinov and Demyanchuk, 2011) are marked by the vertical dashed black lines indicating $2.5\text{--}8.0 \times 10^{-4} \text{ km}^3$ as minimum and maximum volume, respectively. Pyroclastic flow volumes from 0.2 to $2.0 \times 10^{-2} \text{ km}^3$ are given by Girina (this volume) and marked by the vertical solid black lines. These volumes, however, are overestimates in terms of source volume change as they are not a dense rock equivalent and contain unspecified portions of non-juvenile material (i.e., dome material and other lithics).

Using the values for volumes and depths specified above, we would not record any deformation due to a deep spherical source for such small volume changes of Bezymianny eruptions. If any of the eruptions was fed straight from the basaltic layer at 18 km proposed by Fedotov et al. (2010), we would see this only in the vertical component for volume changes $> 0.01 \text{ km}^3$, and would expect to observe this at all stations across the network. As we do not see this, we rule out direct involvement of this source for larger events. A similar

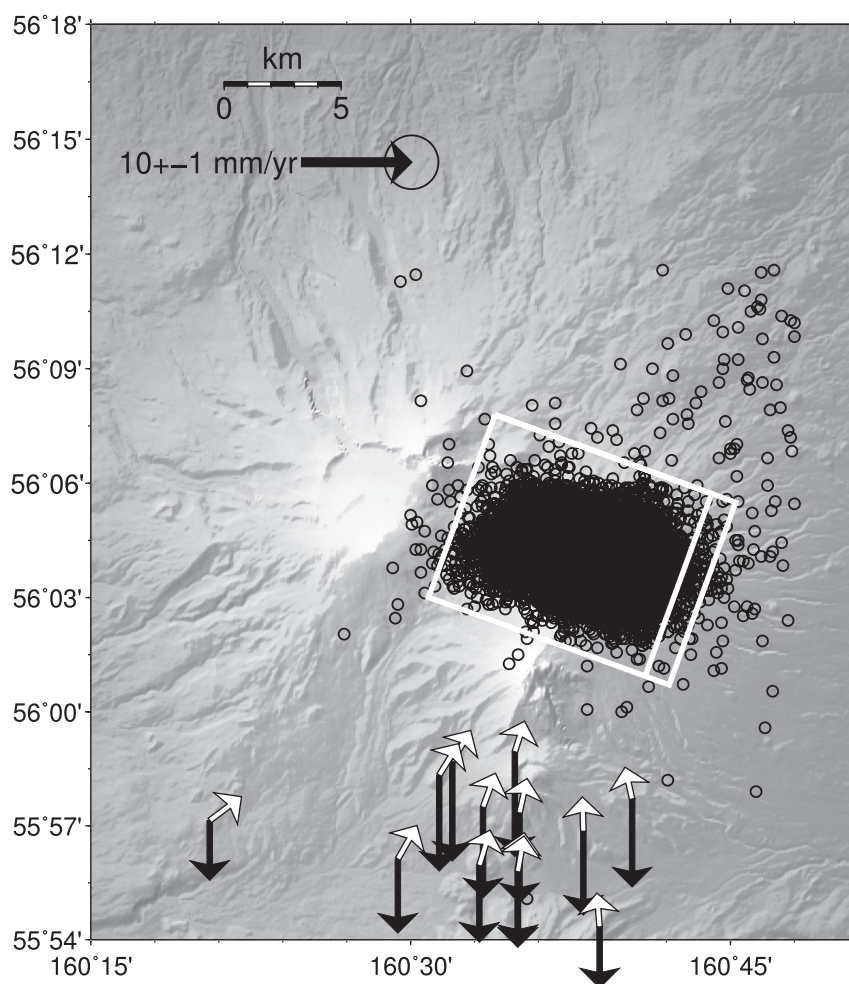


Fig. 9. Sill model (white rectangle, double line indicates down dip end) inferred from seismicity below 22.5 km (black circles). Velocity predictions relative to E1 for this model assuming a closing rate 0.22 m/yr for the sill are shown as white (horizontal) and black (vertical) vectors.

decision follows for sources suspected at 7 and 10 km as we do not observe consistent network wide deformation at times of explosions in both the vertical and the horizontal field.

What we do observe is subtle deformation in the horizontal (north component) at BZ09 only. If we combine the vertical and horizontal contours for the region highlighted in pink in Fig. 11A,B, we get the plot in the inset in Fig. 11A. The area highlighted in red shows the combinations of depth and volume change that would induce 1 cm or more motion in the horizontal at BZ09, but motion at or below the detection limit in the vertical at BZ09 and the horizontal at BZ03. We infer that a pressure point source at 0.25–1.5 km with a volume change of $1\text{--}4 \times 10^{-4} \text{ km}^3$ may be involved in the eruptions. This falls in the region of the shallow source within the edifice as proposed by Thelen et al. (2010). The range of permissible volume changes lies around the lower limit of 1984–2007 lava flow volumes (Zharinov and Demyanchuk, 2011). We emphasize again our assumption that this source is located straight underneath Bezymianny's dome summit at 55.9719° N , 160.5965° E .

A second plausible location for a shallow source is about 2 km to the south-east of the dome where particle motion plots of very long period seismic signals during eruptions on Dec. 16, 2009 (21:46:00 UTC) and May 31, 2010 (12:34:00 UTC) suggest a region involved in the explosive activity (West, this volume). If we repeat the exercise described above for this hypothetical horizontal source location, we get the sensitivity contours shown in Fig. 12. While station BZ02 is most sensitive to this source and hence would be critical to confirm this source location, it was not operating during any of the events

for which West (this volume) hypothesizes this source location. Note that deformation at BZ09 induced by a point source at such a location would likely induce motion in both the east and the north component, rather than just the north component as we observed. More complex scenarios such as a dike could possibly limit the induced motion to the north component, though.

The inset in Fig. 12A shows that a possible pressure point source could be located at 0.25–3.5 km depth changing in volume by about $0.6\text{--}1.5 \times 10^{-3} \text{ km}^3$. These ranges are larger than before because of the increased distance between BZ09 and the source. Note that the depth range inferred for the summit source is included here and that shallower depths require smaller volume changes; i.e. there is a significant depth–volume change trade-off.

5. Discussion

The two striking observations from the GPS data for 2005–2010 are (1) rapid and continuous network wide subsidence, which diminishes in amplitude away from the KGV, but still appears to affect stations more than 40 km away (KLU, MAYS), and (2) the absence of a clear deformation pattern related to individual eruptions at stations other than BZ09 which, prior to and after explosions, shows slight deviations from the average motion in the north component. From our analysis above we infer that a deep sill at about 30 km underneath Kluchevskoy constantly discharges material that may be fed into shallower reservoirs under Bezymianny and Kluchevskoy, respectively. A very shallow reservoir suggested by Thelen et al. (2010), likely

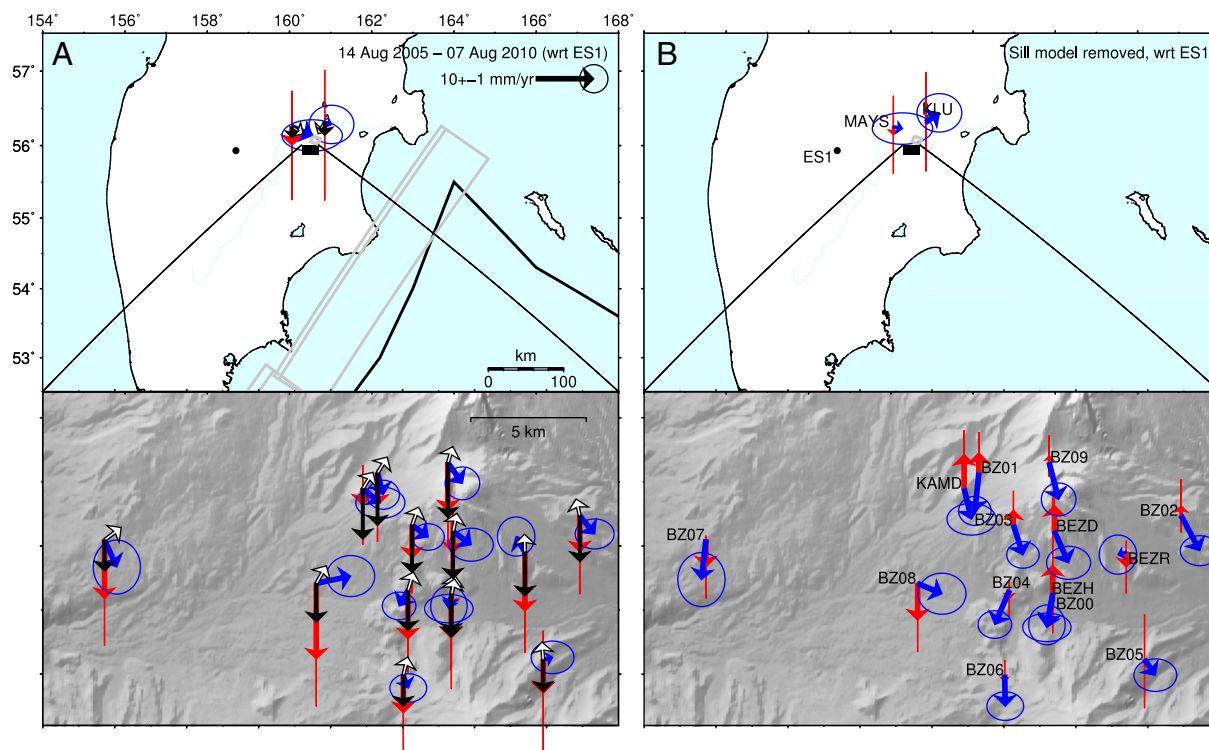


Fig. 10. Site velocities and sill model predictions. (A) Velocities (blue: horizontal, red: vertical) with respect to ES1 (tectonics model removed, load model not removed) and predictions for a deflating sill under the Kluchevskoy Volcano (white: horizontal, black: vertical). (B) Residuals after subtracting the model predictions from the data. The residual horizontal motion may be due to a mid-crustal volcanic source at Kluchevskoy or residual tectonic motion. (For interpretation of the references to color in this figure legend, the reader is referred to the web version of this article.)

within Bezymianny's edifice, appears to explain slight deformation during individual events which seem to be sourced from a mid-crustal reservoir with volume changes at or below the detection limit of our network. In the following we will discuss these findings individually.

5.1. Long-wavelength subsidence: deep sill

The regional extent of the signal and therefore the dimensions of the volcanic source are certainly astonishing, yet similar observations have been made at other volcanoes, for example in South America (Pritchard and Simons, 2004b; Fournier et al., 2010). Those studies benefit from high resolution spatial sampling inherent to InSAR techniques, which clearly show the extent of the deformation. For the KGV, Pritchard and Simons (2004a) report deformation due to the 1975–76 Tolbachik lava flows from satellite data between 1992 and 2003, but cannot resolve deformation due to any of the eruptions at the KGV volcanoes during that period. Poor spatial and temporal coverage limits detection to larger signals in that region (Pritchard and Simons, 2004a). Within the PIRE–Kamchatka project several groups attempted InSAR analysis of more recent data for this region. The results remain similar to those of Pritchard and Simons (2004a). Lack of coherence due to snow cover for much of the year limits success and the small amplitude of the signal over such a large region poses another problem as atmospheric effects show similar behavior and hence make the signal hard to detect.

Various authors (e.g., Fedotov et al., 2010; Koulakov et al., 2011, this volume, and KBGS seismic catalog) have suggested a deep source under Kluchevskoy and, in fact, these findings largely constrain our source parametrization. Formal inversion procedures such as simulated annealing or simple grid searches fail due to the very regional nature of the signal, which is sampled too localized by our network. In combination with a small signal amplitude, or rather, small change in signal amplitude across the network, these methods place the best fitting source at locations not in agreement with previous studies,

observed surface activity, and seismic evidence. However, using the occurrence of seismicity and its spatial features as model constraints (Fig. 8), we are able to limit the fundamental source geometry to a non-spherical source, and our inferred closing rate of the sill suggests a volume change of the source ($0.019\text{--}0.027\text{ km}^3/\text{yr}$) that agrees very well with long term production estimates for the Kluchevskoy Volcano ($0.023\text{ km}^3/\text{yr}$) and is a factor of 2–3 smaller than the long term productivity of the entire group $0.057\text{ km}^3/\text{yr}$ (Fedotov et al., 2010) (converted from their estimate of $150\text{ Gt}/\text{yr}$ assuming a density of 2600 kg m^{-3}).

We should not put too much emphasis on the discrepancy with the productivity of the entire group as Fedotov et al. (2010) estimate this long term trend from all eruptions since 1930, which includes the 1956 Bezymianny eruption and the 1975–76 Great Tolbachik Fissure Eruption; events of a size we did not observe during our study.

A critical point about magma source location estimation is the depth–volume (here opening) trade-off for volcanic sources, meaning that a deep source with a large volume change induces displacements similar to a shallow source with less volume change. This is particularly important when we are not using the full 3-D displacement field. While we constrain the deep sill from seismic observations, Fedotov et al. (2010) also suggest a basaltic layer at about 18 km that may underlie parts of the KGV, which is supported by earthquakes during the 1975–76 Tolbachik eruption. In a test to see whether the source we put under Kluchevskoy would induce similar displacements at shallower depths, we vary depth and opening and calculate the χ^2 misfit between data and each of these sources. Fig. 13 shows that the same source geometry at a depth of 18 km would result in a significantly increased misfit. Shallower sources, of course, would result in an even larger misfit. Therefore, the constraints from seismicity and the inferred opening are robust.

Although we constrained our model based on information provided by other disciplines rather than inverting for the parameters giving the best model fit to the data, the resulting fit of model prediction

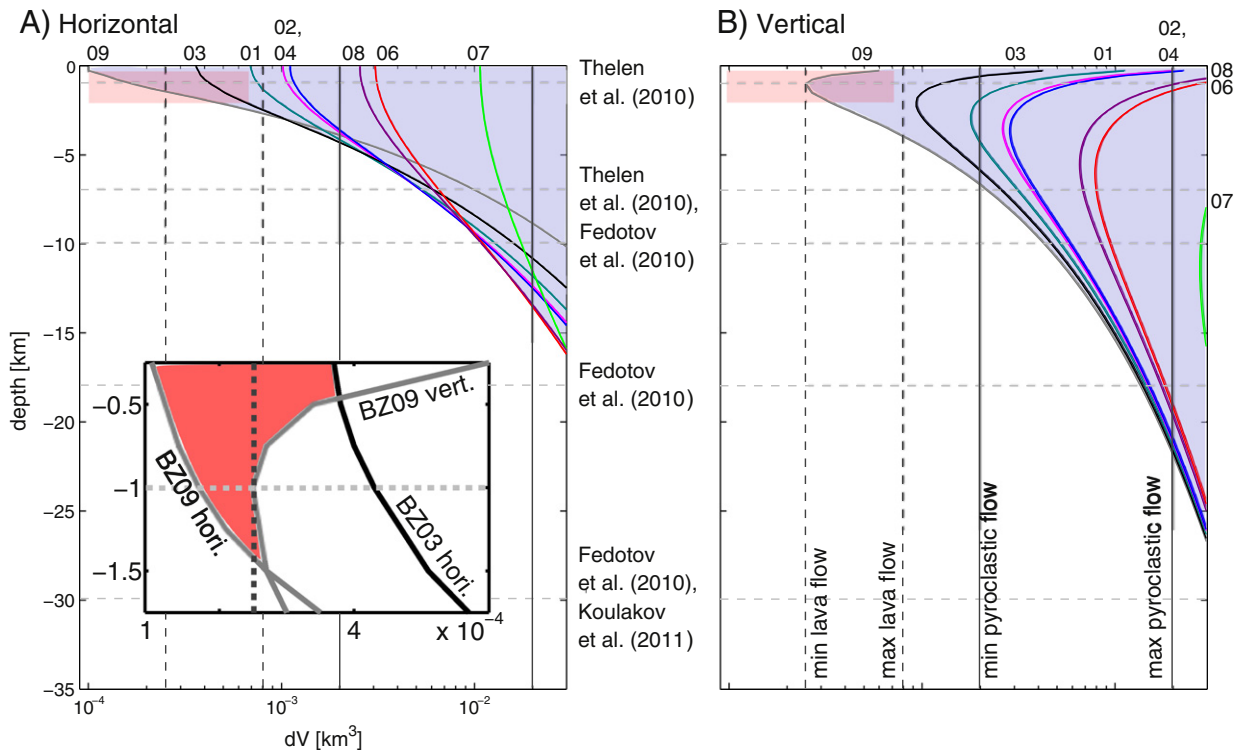


Fig. 11. Network sensitivity assuming a Mogi source under underneath Bezymianny's dome summit at 55.9719° N, 160.5965° E. Contours indicate volume change–depth combinations that would induce at least 1 cm of motion in horizontal (A) and vertical (B) at continuous GPS stations around Bezymianny. As station names only the two digit code is given, the leading “BZ” is left out for clarity. Note that volume change on horizontal axis is given on logarithmic scale. The horizontal gray dashed lines indicate depths of suggested sources; respective references are listed in between the panels. The vertical black dashed lines indicate a range of lava flow volumes extruded during eruptions (lava flows from 1984 to 2007 (Zharinov and Demyanchuk, 2011) $2.5\text{--}8.0 \times 10^{-4} \text{ km}^3$). The solid lines bracket a range of pyroclastic flow deposit volumes ($0.2\text{--}2.0 \times 10^{-2} \text{ km}^3$; Girina, this volume). (A) Inset Combination of vertical and horizontal contours for the region highlighted in pink in panels (A) and (B). The area highlighted in red shows the combinations of depth and volume change that would induce 1 cm or more motion in the horizontal at BZ09, but motion at or below the detection limit in the vertical at BZ09 and the horizontal at BZ03. A pressure point source at 0.25–1.5 km with a volume change of $1\text{--}4 \times 10^{-4} \text{ km}^3$ may be involved in the eruptions which falls in the region of a shallow source within the edifice as proposed by Thelen et al. (2010). (For interpretation of the references to color in this figure legend, the reader is referred to the web version of this article.)

to measurements is fairly good in both vertical and horizontal, i.e. the source generates small horizontal deformation. Subtracting the modeled velocities from the data results in residual horizontal velocities (Fig. 10) that seem to gain coherence and may be explained either with a tectonic feature or maybe a shallower source at Kluchevskoy. An inversion for a point source did not yield any reasonable results. This may be revisited in the future when a better spatial distribution of data is available for this region and surface load effects as well as tectonics are better understood.

An important remaining question is where does all the material, that continuously leaves these deep depths, migrate to? As stated above, the removed volume of material agrees well with the long term eruption rate of the Kluchevskoy Volcano, but neither Kluchevskoy nor Bezymianny erupt continuously. This calls for an additional mid-crustal storage region underneath those two volcanoes, which is suggested by seismicity (Fedotov et al., 2010; Thelen et al., 2010; Koulakov et al., 2011). While we may actually record some long term mid-crustal inflation at Kluchevskoy (Fig. 10), eruptions seem too frequent at Bezymianny to amount to enough detectable deformation (Figs. 11, 12). Additionally, compression and decompression of the magma at mid crustal depths may hide some of the mass transfer and result in less recordable deformation (Johnson et al., 2000; Rivalta and Segall, 2008).

To fully resolve the deep source under the Kluchevskoy Volcano without relying on outside constraints, additional, regionally distributed continuous GPS stations will be necessary. Stations in between Bezymianny and Kluchevskoy, around Kluchevskoy, and in the far field (mainly east of Kluchevskoy and south of Bezymianny, at least 20 km from the volcanoes) are needed to better resolve the spatial

limits of the deep source. GPS sites along the Central Kamchatka Depression, away from volcanic centers, would allow resolution of residual regional and local tectonics whose current contributions are not well quantified. Given the suggested complexity of the subsurface plumbing system of the KGV (Fedotov et al., 2010; Thelen et al., 2010; Koulakov et al., 2011, this volume), the quantity of data must provide spatial and temporal coverage large enough to allow solving for more than one source (Turner et al., this volume) and migrating sources (Koulakov et al., this volume).

5.2. Co-eruptive deformation: shallow reservoir

A very shallow storage region within Bezymianny's edifice was proposed by Thelen et al. (2010). They based this on a small aseismic area inferred from high-resolution earthquake locations and on fluid inclusions in plagioclase rims, which require magma storage at such shallow depths (Thelen et al., 2010, their pers. comm. with P. Izbekov). Since Thelen et al. (2010) only analyzed about 3 months of data from the 2007 eruptive sequence it is unclear whether this region is a transient or permanent feature. López et al. (in press) find evidence for shallow degassing magma in 2007 and 2010. Since the gas samples were collected 1–3 months after the respective eruptions, the magma could have been a residual in the conduit or associated with lava flow effusion [?ópez,?]. On the other hand, this may suggest a more long-lived shallow reservoir, or at least an episodically active feature. Due to the repetitive nature of the slight eruption related deformation in the north component of BZ09 during our observation period of 5 years, we suggest that this may be a more permanent feature.

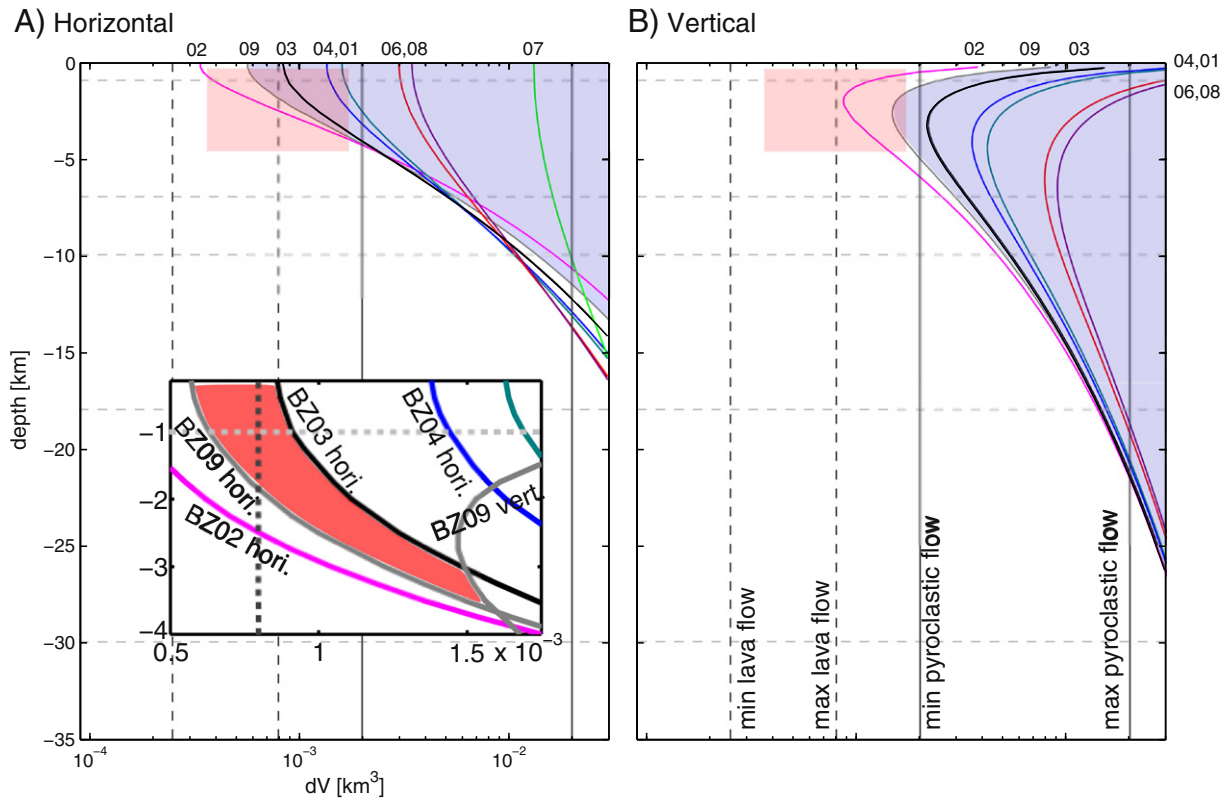


Fig. 12. Similar to Fig. 11, but for a source suggested by West (this volume) in the blast zone about 2 km SE of the dome. Note that BZ02 was not operational during the two times (Dec. 16, 2009 and May 31, 2010) this source is assumed to have been active.

However, future improved observations with more sensitive instruments are necessary to answer this question with more certainty.

The volume changes of this storage region are near the detection limit of the network and are small compared to the volume of erupted products; comparable to or smaller than the smallest 1984–2007 lava

flows even (Fig. 11A,inset). This discrepancy between erupted material and apparent lack of volume change can be explained in several ways. Rivalta and Segall (2008) suggest that after the removal of material from a pressurized, volatile rich magma, the lost volume is simply recovered through expansion of volatiles. This seems to work only in a closed system though, as volatiles may simply escape during time of shallow storage when the system is open. As Bezymianny is an open system and constantly degassing, this pressure build-up might not occur.

Another possibility for volume-loss recovery is recharging of the shallow reservoir with material from depth (e.g., Grapenthin et al., in press-a), or direct evacuation of material mostly from deeper regions, which seems supported by Turner et al. (this volume) who model major and trace element as well as mineral data as a mixing of three different magmas. If the bulk of the material came from deeper (8–10 km) where Thelen et al. (2010), Fedotov et al. (2010), and Turner et al. (this volume) suggest an intermediate storage region, the removal of magma at these depths could happen at network detection limits (Fig. 11) and still agree with volumes of erupted material. This easily explains the lack of volume change in the shallow reservoir.

The fact that West (this volume) recognizes small amplitude deformation in the seismic data located about 2 km to the south-east of Bezymianny's dome in the 1956 blast zone for eruptions in late 2009 and May 2010 deserves some attention. We do not think that this is an actual shallow storage region as BZ09 shows deformation similar to prior events which is limited to the north component only. A very specific source geometry would be necessary to induce such deformation from this distance, which we consider unlikely. Deformation inferred from broadband seismometers suggests sub-mm displacements, though, which GPS cannot detect. An explanation may be the transient pathways of fluid migration as opposed to well established conduit systems suggested by Koulakov et al. (this volume). An improved record at BZ02 could help to clarify this (Fig. 12).

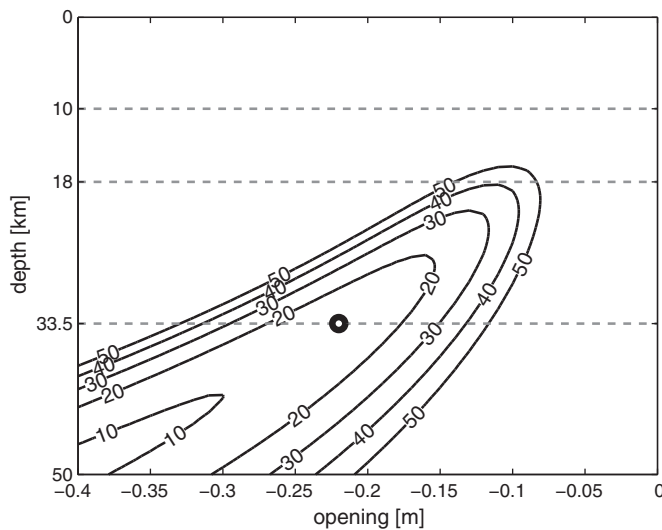


Fig. 13. Sill depth-opening-trade-off in χ^2 misfit space. Bold circle marks the best opening derived for the sill we constrained from seismicity at 33.5 km depth. Other likely source locations are marked with dotted lines. If the width and length are kept fixed and we change just the opening, the shallower locations are unlikely sources for the deflation source. Note that the selected source does not provide the best fit to the data, which would be below 50 km; probably to accommodate the larger signal observed at BZ07. Stations used: BZ00, BZ01, BZ02, BZ04, BZ05, BZ06, BZ07, BEZR, MAYS, KLU.

6. Conclusions

Continuous and campaign GPS observations in a dense network of stations around the Bezymianny Volcano, Kamchatka, show continuous subsidence at rapid rates between 8 and 12 mm/yr. This signal may range as far as about 40 km to the north (Kluchi) and to the east (Mayskoye) where we observe 4.3 and 5.3 mm/yr of subsidence, respectively. In time, this subsidence may be traced back to 1978–87 as an earlier study by Fedotov et al. (1992) suggests similar broad subsidence, although at smaller rates. Tectonic deformation related to the build-up of interseismic strain due to the subduction of the Pacific plate to the east induces significant horizontal deformation in the network. According to the model of Bürgmann et al. (2005) vertical deformation due to subduction is negligible. A first order model of surface loading by eruptive products of the KGV explains a fraction of the subsidence signal and suggests that this signal source is non-negligible and future work should focus on deriving a better constrained Earth and load model for this region. The bulk of the vertical signal, however, is explained by a sill-like source under Kluchevskoy. This sill is at about 30 km depth, dips 13° to the south-east, and is about 9.5 km wide and 12.7 km long. We infer a closing rate of 0.22 m/yr, which results in a volume loss of 0.027 km³ (0.16 m/yr and 0.019 km³ considering surface loading). Additional stations in the near and far field are required to fully resolve the spatial extent and likely partitioning of this source.

From network sensitivity analysis, we limit the possible sources underneath the summit of Bezymianny that can induce slight deformation at BZ09 only to a shallow reservoir at about 0.25–1.5 km depth with a volume change of 1–4 × 10⁻⁴ km³. Much of the material erupted at Bezymianny may be sourced from deeper mid-crustal reservoirs with co-eruptive volume changes at or below the detection limit of the GPS network. Installation of more sensitive instruments such as tiltmeters would lower the detection limit of the network and hence allow resolving more subtle co-eruptive motion.

Supplementary data to this article can be found online at <http://dx.doi.org/10.1016/j.jvolgeores.2012.11.012>.

Acknowledgments

We want to thank the many individuals who were involved in the PIRE-Kamchatka project. Many people contributed to solve the plethora of issues that come up in realizing such a large project in such a remote location. Institutional support through IVS and KBGS was crucial for the success of this project. Sergey Ushakov of IVS ably managed the Russian side of the field program. We especially thank Pavel Izbekov (University of Alaska Fairbanks) for his ideas and criticisms offered in many discussions on the Bezymianny Volcano. Mike West (University of Alaska Fairbanks) provided earthquake locations, which we used to constrain our model. Judith Levy (University of Alaska Fairbanks) provided us with the digital elevation model used for our maps. Taryn López provided useful comments on the manuscript. We also want to thank all other colleagues who are part of the PIRE-Kamchatka project for insightful, interdisciplinary discussions of data from this project. Efforts and comments by Editor Malcom Rutherford and Guest Editor Mike West as well as two anonymous reviewers improved the manuscript and are gratefully acknowledged. Most of the figures were created using the GMT public domain software (Wessell and Smith, 1995). This work was supported by NSF grant 0530278.

References

Anderson, E.M., 1936. The dynamics of the formation of cone-sheets, ring-dykes, and caldron-subsidences. *Proceedings of the Royal Society of Edinburgh* 56, 128–157.
 Apel, E., Bürgmann, R., Steblöv, G.M., Vasilenko, N., King, R., Prytkov, A., 2006. Independent active microplate tectonics of northeast Asia from GPS velocities and block modeling. *Geophysical Research Letters* L11303. <http://dx.doi.org/10.1029/2006GL026077>.

Argus, D.F., Gordon, R.G., Heflin, M.B., Ma, C., Eanes, R.J., Willis, P., Peltier, W.R., Owen, S.E., 2010. The angular velocities of the plates and the velocity of Earth's centre from space geodesy. *Geophysical Journal International* 913–960. <http://dx.doi.org/10.1111/j.1365-246X.2009.04463.x>.
 Battaglia, M., Cervelli, P.F., Murray-Muraleda, J.R., in press. Modeling Crustal Deformation: A Catalog of Deformation Models and Modeling Approaches. United States Geological Survey. Professional Paper.
 Belousov, A., Voight, B., Belousova, M., 2007. Directed blasts and blast-generated pyroclastic density currents: a comparison of the Bezymianny 1956, Mount St Helens 1980, and Soufrière Hills, Montserrat 1997 eruptions and deposits. *Bulletin of Volcanology* 701–740. <http://dx.doi.org/10.1007/s00445-006-0109-y>.
 Bürgmann, R., Kogan, M.G., Steblöv, G.M., Hilley, G., 2005. Interseismic coupling and asperity distribution along the Kamchatka subduction zone. *Journal of Geophysical Research* 110, B07405. <http://dx.doi.org/10.1029/2005JB003648>.
 Carter, A.J., Ramsey, M.S., Belousov, A.B., 2007. Detection of a new summit crater on Bezymianny Volcano lava dome: satellite and field-based thermal data. *Bulletin of Volcanology* 811–815. <http://dx.doi.org/10.1007/s00445-007-0113-x>.
 Cervelli, P., Murray, M.H., Segall, P., Aoki, Y., Kato, T., 2001. Estimating source parameters from deformation data, with an application to the March 1997 earthquake swarm off the Izu Peninsula, Japan. *Journal of Geophysical Research* 11,217–11,237.
 Fedotov, S.A., Markhinin, Y.K. (Eds.), 1983. *The Great Tolbachik Fissure Eruption*. Cambridge University Press, Cambridge. <http://dx.doi.org/10.1134/S074204631001001X>.
 Fedotov, S.A., Zharinov, N.A., Gontovaya, L.I., 2010. The magmatic system of the Klyuchevskaya group of volcanoes inferred from data on its eruptions, earthquakes, deformation, and deep structure. *Journal of Volcanology and Seismology* 4, 3–35.
 Fedotov, S.A., Zharinov, N.A., Sharoglazova, G.A., Demianchuk, Y.V., 1992. Deformations of the Earth's surface in the Klyuchi geodynamic polygon, Kamchatka, 1978–1987. *Tectonophysics* 151–156.
 Fournier, T.J., Pritchard, M.E., Riddick, S.N., 2010. Duration, magnitude, and frequency of subaerial volcano deformation events: new results from Latin America using InSAR and a global synthesis. *Geochemistry, Geophysics, Geosystems* Q01103. <http://dx.doi.org/10.1029/2009GC002558>.
 Freymueller, J.T., Kaufman, A.M., 2010. Changes in the magma system during the 2008 eruption of Okmok volcano, Alaska, based on GPS measurements. *Journal of Geophysical Research* B12415. <http://dx.doi.org/10.1029/2010JB007716>.
 Freymueller, J.T., Woodard, H., Cohen, S.C., Cross, R., Elliott, J., Larsen, C.F., Hreinsdóttir, S., Zweck, C., 2008. Active deformation processes in Alaska, based on 15 years of GPS measurements. In: Freymueller, J.T., Haeussler, P.J., Wesson, R.L., Ekström, G. (Eds.), *Active Tectonics and Seismic Potential of Alaska*. Geophysical Monograph. AGU, pp. 1–42.
 Fu, Y., Freymueller, J.T., 2012. Seasonal and long-term vertical deformation in the Nepal Himalaya constrained by GPS and GRACE measurements. *Journal of Geophysical Research* B03407. <http://dx.doi.org/10.1029/2011JB008925>.
 Girina, O. A., this volume. Chronology of Bezymianny Volcano activity in 1956–2010. *Journal of Volcanology and Geothermal Research*.
 Gorskov, G., 1959. Gigantic eruption of volcano Bezymianny. *Bulletin of Volcanology* 77–109.
 Grapenthin, R. (2007). *CrusDe: A plug-in based simulation framework for composable CRUSTal DEformation simulations using Green's functions*. Master's thesis.
 Grapenthin, R., Freymueller, J. T., & Kaufman, A. M., in press-a. Geodetic observations during the 2009 eruption of Redoubt Volcano, Alaska. *Journal of Volcanology and Geothermal Research*. <http://dx.doi.org/10.1016/j.jvolgeores.2012.04.021>.
 Grapenthin, R., Ofeigsson, B.G., Sigmundsson, F., Sturkell, E., 2010. Pressure sources versus surface loads: Analyzing volcano deformation signal composition with an application to Hekla volcano, Iceland. *Geophysical Research Letters* 37, L20310. <http://dx.doi.org/10.1029/2010GL044590>.
 Gregorius, T., 1996. *GIPSY OASIS II: How It Works*. University of Newcastle upon Tyne: self.
 Johnson, D.J., Sigmundsson, F., Delaney, P.T., 2000. Comment on "Volume of magma accumulation or withdrawal estimated from surface uplift or subsidence, with application to the 1960 collapse of Kilauea volcano". In: Delaney, P.T., McTigue, D.F. (Eds.), *Bulletin of Volcanology*, pp. 491–493.
 Koulakov, I., Gordeev, E.I., Dobretsov, N.L., Vernikovskiy, V.A., Senyukov, S., Jakovlev, A., 2011. Feeding volcanoes of the Kluchevskoy group from the results of local earthquake tomography. *Geophysical Research Letters* L09305.
 Koulakov, I., Gordeev, E. I., Dobretsov, N. L., Vernikovskiy, V. A., Senyukov, S., Jakovlev, A., & Jaxybulatov, K., this volume. Variable feeding regimes of the Kluchevskoy group volcanoes (Kamchatka, Russia) derived from time-dependent seismic tomography. *Journal of Volcanology and Geothermal Research*.
 López, T. M., Ushakov, S., Izbekov, P., Tassi, F., Werner, C., & Cahill, C., in press. Constraints on magma processes, subsurface conditions, and total volatile flux at Bezymianny Volcano in 2007–2010 from direct and remote volcanic gas measurements. *Journal of Volcanology and Geothermal Research*, in review. <http://dx.doi.org/10.1016/j.jvolgeores.2012.10.015>.
 Malyshev, A.I., 2000. *Life of the Volcano*. (in Russian) Ural Division of the Russian Academy of Sciences.
 Mogi, K., 1958. Relations between eruptions of various volcanoes and the deformations of the ground surface around them. *Bulletin. Earthquake Research Institute, University of Tokyo* 36, 99–134.
 Okada, Y., 1992. Internal deformation due to shear and tensile faults in a half-space. *Bulletin of the Seismological Society of America* 1018–1040.
 Pinel, V., Sigmundsson, F., Sturkell, E., Geirsson, H., Einarsson, P., Gudmundsson, M.T., Högnadóttir, T., 2007. Discriminating volcano deformation due to magma movements and variable surface loads: application to Katla subglacial volcano, Iceland.

- Geophysical Journal International 169, 325–338. <http://dx.doi.org/10.1111/j.1365-246X.2006.03267.x>.
- Pritchard, M.E., Simons, M., 2004a. Surveying volcanic arcs with satellite radar interferometry: the central Andes, Kamchatka, and beyond. *GSA Today* 14. [http://dx.doi.org/10.1130/1052-5173\(2004\)014<4:SWAWSR>2.0.CO;2](http://dx.doi.org/10.1130/1052-5173(2004)014<4:SWAWSR>2.0.CO;2).
- Pritchard, M.E., Simons, M., 2004b. An InSAR-based survey of volcanic deformation in the central Andes. *Geochemistry, Geophysics, Geosystems* Q02002. <http://dx.doi.org/10.1029/2003GC000610>.
- Rivalta, E., Segall, P., 2008. Magma compressibility and the missing source for some dike intrusions. *Geophysical Research Letters* L04306. <http://dx.doi.org/10.1029/2007GL032521>.
- Savage, J.C., 1983. A dislocation model of strain accumulation and release at a subduction zone. *Journal of Geophysical Research* 4984–4996.
- Shestakov, N.V., Gerasimenko, M.D., Takahashi, H., Kasahara, M., Bormotov, V.A., Bykov, V.G., Kolomiets, A.G., Gerasimov, G.N., Vasilenko, N.F., Prytkov, A.S., Timofeev, V.Y., Ardyukov, D.G., Kato, T., 2011. Present tectonics of the southeast of Russia as seen from GPS observations. *Geophysical Journal International* 184, 529–540. <http://dx.doi.org/10.1111/j.1365-246X.2010.04871.x>.
- Thelen, W., West, M., Senyukov, S., 2010. Seismic characterization of the fall 2007 eruptive sequence at Bezymianny Volcano, Russia. *Journal of Volcanology and Geothermal Research* 194, 201–213. <http://dx.doi.org/10.1016/j.jvolgeores.2010.05.010>.
- Turcotte, D.L., Schubert, G., 2002. *Geodynamics*. Cambridge University Press.
- Turner, S. J., Izbekov, P., & Langmuir, C., this volume. The magma plumbing system of Bezymianny Volcano: Insights from trace element whole-rock geochemistry and amphibole compositions. *Journal of Volcanology and Geothermal Research*.
- Wessel, P., Smith, W.H.F., 1995. New version of the generic mapping tools released. *EOS Transactions AGU* 76, 329.
- West, M. E., this volume. Recent eruptions at Bezymianny volcano – a seismic comparison. *Journal of Volcanology and Geothermal Research*.
- Williams, S.D.P., 2008. CATS: GPS coordinate time series analysis software. *GPS Solutions* 147–153. <http://dx.doi.org/10.1007/s10291-007-0086-4>.
- Yamakawa, N., 1955. On the strain produced in a semi-infinite elastic solid by an interior source of Stress. *Zisin Journal of the Seismological Society of Japan* 84–98.
- Yang, X.M., Davis, P.M., Dieterich, J.H., 1988. Deformation from inflation of a dipping finite prolate spheroid in an elastic half-space as a model for volcanic stressing. *Journal of Geophysical Research* 4257–4549.
- Zharinov, N.A., Demyanchuk, Y.V., 2011. Assessing the volumes of material discharged by Bezymianny Volcano during the 1955–2009 period. *Journal of Volcanology and Seismology* 5, 100–113.
- Zumberge, J.F., Heflin, M.B., Jefferson, D.C., Watkins, M.M., Webb, F.H., 1997. Precise point positioning for the efficient and robust analysis of GPS data from large networks. *Journal of Geophysical Research* 5005–5017.